

LIGHT TRIGGERED SELF-ASSEMBLY AND HYDROGELATION OF
AZOBENZENE BEARING PEPTIDES AND INVESTIGATION OF THEIR
NANOSTRUCTURES

A THESIS SUBMITTED TO
THE GRADUATE SCHOOL OF NATURAL AND APPLIED SCIENCES
OF
MIDDLE EAST TECHNICAL UNIVERSITY

BY

MENİZ TEZCAN

IN PARTIAL FULFILLMENT OF THE REQUIREMENTS
FOR
THE DEGREE OF MASTER OF SCIENCE
IN
CHEMISTRY

SEPTEMBER2013

Approval of the thesis:

LIGHT TRIGGERED SELF-ASSEMBLY AND HYDROGELATION OF
AZOBENZENE BEARING PEPTIDES AND INVESTIGATION OF THEIR
NANOSTRUCTURES

submitted by **MENİZ TEZCAN** in partial fulfillment of the requirements for the degree of
Master of Science in Chemistry Department, Middle East Technical University by,

Prof. Dr. Canan Özgen
Dean, Graduate School of **Natural and Applied Sciences**

Prof. Dr. İlker Özkan
Head of Department, **Chemistry**

Assist. Prof. Dr. Salih Özçubukçu
Supervisor, **Chemistry Dept., METU**

Examining Committee Members:

Prof. Dr. Cihangir Tanyeli
Chemistry Dept., METU

Assist. Prof. Dr. Salih Özçubukçu
Chemistry Dept., METU

Prof. Dr. Engin Umut Akkaya
Chemistry Dept., Bilkent University

Prof. Dr. Ceyhan Kayran
Chemistry Dept., METU

Assist. Prof. Dr. İrem Erel Göktepe
Chemistry Dept., METU

Date:03.09.2013

I hereby declare that all information in this document has been obtained and presented in accordance with academic rules and ethical conduct. I also declare that, as required by these rules and conduct, I have fully cited and referenced all material and results that are not original to this work.

Name, Last name: Meniz Tezcan

Signature:

ABSTRACT

LIGHT TRIGGERED SELF-ASSEMBLY AND HYDROGELATION OF AZOBENZENE BEARING PEPTIDES AND INVESTIGATION OF THEIR NANOSTRUCTURES

Tezcan, Meniz

M.Sc., Department of Chemistry

Supervisor: Assist. Prof. Dr. Salih Özçubukçu

September 2013, 55 pages

Since their serendipitously discovery in 1993, hydrogel of self-assembling peptides are becoming an emerging field especially in last 10 years. For their application in selective drug delivery, tissue engineering and biomedical applications, divergent peptide libraries can be constructed through chemical peptide synthesis, utilizing synthetic amino acids addition to 21 naturally occurring ones. One of the methods which were applied to obtain self-assembling peptides is incorporating strongly beta-sheet forming amino acids in the sequence of peptides. These peptides having strong beta-sheet structures can undergo self-assembly and form nano fibers resulting a hydrogel character as a macroscopic property under certain conditions. For the application of hydrogel forming peptides, self-assembly should be stimulus responsive and preferably reversible process.

The target of this project is to obtain a light controlled self-assembly and hydrogelation of peptides in order to use in biomedical and biotechnological applications. For this purpose, initially, an azobenzene amino acid derivative that can respond to stimuli synthesized using coupling reaction. After the synthesis, including artificial azobenzene amino acid in the middle of peptide sequence; mainly Lysine (K), Alanine (A) / Phenylalanine (F) and Glutamic acid (E) are preferred among the natural amino acids. It is shown that the peptide composed of those mentioned amino acids can respond light. Utilizing the change in geometry and polarity of azobenzene upon irradiating with light, a control in the self-assembly and hydrogelation of the peptide is the target of this project. With the unique design of this system and its photochemical isomerization, hydrogel structure is disrupted and this feature can be used as a selective drug delivery system.

Keywords: Amino acid, peptide hydrogels, SPPS, stimuli-responsiveness, azobenzene.

ÖZ

IŞIKLA TETİKLENEREK KENDİLİĞİNDENYAPILANAN AZOBENZEN İÇERİKLİ PEPTİT HİDROJELLERVENANOYAPILARININ İNCELENMESİ

Tezcan, Meniz
Yüksek Lisans, Kimya Bölümü
Tez Yöneticisi: Yrd. Doç. Dr. Salih Özçubukçu

Eylül 2013, 55 sayfa

1993 yılında tesadüfi keşiflerinin ardından, kendiliğindenyapılanarak hidrojel oluşturabilenpeptitler özellikle son 10 yılın hızlagelişen alanlarından biri olmuştur.Seçici ilaç salınımı, doku mühendisliği vebiyomedikal uygulamalarda kullanılabilmeleri için doğada bulunan 21 aminoasite ek, sentetik aminoasitlerden de yararlanarak, birbirinden farklı yapıda birçok peptit kimyasal sentez yöntemleriyle kolaylıkla oluşturulabilir. Peptitleri oluşturan aminoasitlerin çeşitliliği, çok farklı fiziksel ve kimyasal özelliğe sahip peptit yapılarının elde edilmesine olanak sağlamaktadır ve bu sayede de çok daha farklı uygulamalar yapılabilmektedir. Kendi kendine yapılanarak hidrolej oluşturan peptit eldesinde tercih edilen yöntemlerden biri de peptit diziliminde kuvvetli bir şekilde “*beta-sheet*” yapısı oluşturabilen aminoasitlerin kullanılmasıdır. Bu yolla kuvvetli *beta-sheet* oluşturan peptitler, makroskopik boyutta hidrolej özelliği taşımak üzere çeşitli nano-yapılar oluşturabilirler ve bu sürecin tersinir olması da beklenen bir durumdur.

Bu çalışmanın amacı ışıkla tetiklenerek kendiliğinden hidrolel oluşturabilen azobenzen içerikli peptit yapılarının eldesi ve bunların nano yapılarının/biyomalzeme uygulamalarının çalışılmasıdır. Bu amaç doğrultusunda, öncelikle azobenzen türevi içeren bir aminoasit kenetlenme tepkimesiyle sentezlenmiştir. Sentezlenen peptitin kuvvetli bir şekilde moleküller arası “*beta-sheet*” oluşturabilmesi için kullanılan aminoasitlerin dizilimi büyük önem kazanmaktadır. Azobenzen türevi aminoasit dizilimin ortasında olacak şekilde özellikle lizin(K), fenilalanin(F)/ alanin(A), ve glutamik asit (E), bu çalışmada tercih edilmiştir. Azobenzenin kimyasal özelliklerinden de yararlanarak (geometri, polarite vb.) peptitin ışıkla uyarıldığında hidrojel oluşumu ve sistemin fotokimyasal izomerizasyonu bu çalışmanın temelini oluşturmaktadır. Bu sayede oluşturulan sistem seçici ilaç salınımında da kullanılabilir olacaktır.

Anahtar Kelimeler: Amino asit, peptit hidrojel, SPPS, uyarıcı duyarlı, azobenzen.

To my beloved mother and father

ACKNOWLEDGEMENTS

I would like to express my sincere appreciation to my supervisor Assist. Prof. Dr. Salih Özçubukçu. I would like to thank him for his precious guidance and support. It would have been impossible for me to accomplish the work without his patience and encouragement. It was an honor for me to be first graduate student in his research laboratory and I believe his scientific contributions will feed me throughout my whole life.

I also would like to express my appreciation to all of those with whom I have had the pleasure to work within the past two years. I am sincerely grateful to my labmates Güzide Aykent, Gözde Eşan, Burçe Çifçi and Ulvi Oral Karaca for their support, and helpful discussions throughout my studies as well as their kind friendship.

I have received great support from Şevki Can Cevher and would like to thank him for his company and valuable friendship.

I would like to thank my beloved friend Billur Arslan for her endless support, understanding and moral support especially in the last two years. She has been always helpful for re-gaining encouragement.

During the course of this project, I have received great support from Yiğit Altay and want to thank him for all of his precious ideas and helps especially in UNAM laboratories. Other than being a good collaborator, he has always shared his creativity in every step of my life which makes me very grateful for meeting him.

Last but not the least; I would like to thank my family especially my mother Filiz Tezcan, father Cavit Tezcan and my brother Arda Tezcan for their endless love, support and affection throughout my whole life. The completion of this study would not have been possible without them.

TABLE OF CONTENTS

ABSTRACT.....	v
ÖZ.....	vi
ACKNOWLEDGEMENTS.....	viii
TABLE OF CONTENTS.....	ix
LIST OF TABLES.....	xi
LIST OF FIGURES.....	xiii
LIST OF ABBREVIATIONS.....	xv
CHAPTERS.....	1
1.INTRODUCTION.....	1
1.1 Chemistry of Peptides.....	1
1.1.1 Definition and Structural Properties.....	1
1.1.2 Secondary Structures.....	3
1.2 Peptide Hydrogels.....	5
1.2.1 Self-Assembly.....	6
1.2.2 Formation of Structural Motifs in Peptides & Proteins.....	7
1.2.3 Stimuli Responsive Peptide Hydrogels.....	10
1.2.4 Examples for Stimuli Driven Peptide Hydrogels.....	10
1.3 Solid Phase Peptide Synthesis (SPPS).....	13
1.3.2 Reactions & Mechanisms.....	15
1.4 Photochemistry of Azobenzene.....	16
1.4.1 Electronic Absorption Spectra and Excited States.....	16
1.4.2 Cis/Trans Isomerization.....	18
1.4.3 Azobenzenephtoswitches.....	19
1.5 Aim of the Study.....	21
2.RESULTS AND DISCUSSION.....	23
3.CONCLUSION.....	33
4.EXPERIMENTAL.....	35
4.1 Materials and Methods.....	35
4.1.1 Nuclear Magnetic Resonance.....	35
4.1.2 HPLC.....	35

4.1.3 LC-MS-QTOF	35
4.1.4 Photoirradiation	36
4.1.5 Circular Dichroism	36
4.1.6 Scanning Electron Microscope	36
4.1.7 Transmission Electron Microscope	36
4.2 Synthesis of (9H-fluoren-9-yl)methyl 3-aminobenzylcarbamate (Compound 1)	36
4.3 Synthesis of (9H-fluoren-9-yl)methyl 4-aminobenzylcarbamate (Compound 2)	37
4.4 Synthesis of 3-nitrosobenzoic acid (Compound 3)	37
4.4 Synthesis of [3-(3'-(9-Fluorenylmethoxycarbonylamino)methyl)phenylazo]benzoic acid(Compound 4)	38
4.5 Synthesis of [3-(4'-(9-Fluorenylmethoxycarbonylamino)methyl)phenylazo]benzoic acid(Compound 5)	38
4.6 General Procedure for Solid Phase Peptide Synthesis	39
REFERENCES	41
APPENDICES	45
A. LIST OF 21 AMINO ACIDS FOUND IN NATURE	45
B. HR-MS PROFILES	49
C. HPLC PROFILES	51

LIST OF TABLES

TABLES

Table 1.pK values of 20 standard amino acids.	7
Table 2.Results of charge distribution in a peptide with same amino acid recipe.	9
Table 3.(XKXE) ₂ peptide sequences, hydrophobicity, and secondary structure propensity. (^a Amino acid hydrophobicity based on water-octanol partition coefficients relative to Gly. ^b Propensity to occur in β -Sheet secondary structures.) ..	9
Table 4.Types of buffer and adjusted pH values tested for the solubility of <i>Peptide 3</i>	29
Table 5.Designed peptides for light triggered self-assembly.....	30

LIST OF FIGURES

FIGURES

Figure 1. Chemical structure of peptides	1
Figure 2. Resonance stabilization of the peptide bond	2
Figure 3. Peptide and protein structures in increasing order of their complexity.	3
Figure 4. Torsion angles ϕ , ψ and ω	4
Figure 5. Typical hydrogen bond in peptides and proteins.	4
Figure 6. Peptide and protein secondary structures: A) α -helix, B) parallel β -sheets, C) antiparallel β -sheets and D) turn.	5
Figure 7. a) A $\beta\alpha\beta$ motif, b) a β hair pin motif and c) an $\alpha\alpha$ motif.	5
Figure 8. Ionization state of amino acids.	8
Figure 9. Schematic representation of the cyclic to linear peptide conformational switch using a reductive trigger.	11
Figure 10. a) CD spectra of cyclized and reduced (linear) form of peptide. (b) TEM image of fibrillar linear peptide.	11
Figure 11. a) Proposed mechanism of metal-triggered folding and self-assembly. b) Primary sequences of Zn-beta hairpin peptide and the control peptide. c) Structure of the non-natural amino acid <i>1</i> (3-amidoethoxyaminodiacetoxy-2-aminopropionic acid).	12
Figure 12. (a) Light induced material formation. (b) Sequences of carboxyamided peptides.	13
Figure 13. Schematic representation of solid phase peptide synthesis employed with Fmoc chemistry.	14
Figure 14. N-Fmoc Deprotection mechanism.	15
Figure 15. C-terminus activation via HBTU-DIEA mechanism.	16
Figure 16. (E) and (Z) isomers of azobenzene.	17
Figure 17. Schematic MO diagram for Azobenzene.	17
Figure 18. Proposed Mechanisms for Cis/Trans isomerization of azobenzene.	18
Figure 19. a) Optical images of photo-induced phase change of hydrogels formed by azo-Gln-Phe-Ala. b) UV-spectrum of the same hydrogel, before (red solid line) and after (black dash line) UV irradiation. c) HPLC monitoring of the hydrogel, before (upper) and after (lower) photo-induced phase change.	19
Figure 20. Cross-eyed superposition of the 10 best structures of the azobenzene containing peptide derived from GB1 protein.	20
Figure 21. Schematic diagram of photochemical isomerization of azobenzene containing peptides.	21
Figure 22. Structures of azobenzene containing artificial amino acids.	23
Figure 23. Structure of <i>Peptide 1</i> with sequence EFKF-Azo _(3,3) -FKFE.	24
Figure 24. Structure of <i>Peptide 2</i> with sequence EFKF-Azo _(3,4) -FKFE.	24
Figure 25. HPLC chromatogram of azobenzene containing <i>peptide 1</i>	25
Figure 26. CD Spectrum of <i>Peptide 1</i>	26
Figure 27. TEM images of <i>Peptide 1</i> : EFKF-Azo _(3,3) -FKFE. (Before UV on the left and after UV on the right side).	26

Figure 28.SEM images of <i>Peptide 2</i> : EFKF-Azo _(3,4) -FKFE (Before UV on the left and after UV on the right side).....	27
Figure 29.CD Spectrum and TEM images of <i>Peptide 2</i> : EFKF-Azo _(3,4) -FKFE (Before UV on the left and after UV on the right side).....	27
Figure 30.Structure of <i>Peptide 3</i> with sequence EFKF ₂ EFKF-Azo _(3,4) -FKF ₂ EFKF..	28
Figure 31.Structure of <i>Peptide 4</i> with sequence AEAK-Azo _(3,4) -KAEA.....	29
Figure 32. Structure of <i>Peptide 5</i> with sequence of AEAEAKAK-Azo _(3,4) -KAKAEAEA.....	30
Figure 33.CD spectrum of <i>Peptide 4</i>	31
Figure 34.CD Spectrum of <i>Peptide 5</i>	31
Figure 35.TEM image of <i>Peptide 5</i> (before UV irradiation).	32
Figure 36.TEM images of <i>Peptide 5</i> (after UV irradiation).....	32

LIST OF ABBREVIATIONS

Azo _(3,3)	: Azobenzene containing artificial amino acid ([3-(3'-(9-Fluorenylmethoxycarbonylamino)methyl)phenylazo]benzoic acid)
Azo _(3,4)	: Azobenzene containing artificial amino acid ([3-(4'-(9-Fluorenylmethoxycarbonylamino)methyl)phenylazo]benzoic acid)
Boc	: Butyloxycarbonyl
CD	: Circular Dichroism
DCM	: Dichloromethane
DMF	: N,N-Dimethylformamide
DIPEA	: N,N-Diisopropylethylamine
Et ₂ O	: Diethyl ether
Fmoc	: Fluorenylmethyloxycarbonyl
Fmoc-OSu	: <i>N</i> -(9-Fluorenylmethoxycarbonyloxy)succinimide
HBTU	: 2-(1H-Benzotriazole-1-yl)-1,1,3,3-tetramethyluronium hexafluorophosphate
HPLC	: High Performance Liquid Chromatography
LC-MS	: Liquid Chromatography–Mass Spectrometry
MTBE	: Methyl tert-butyl ether
NMR	: Nuclear Magnetic Resonance Spectroscopy
SEM	: Scanning Electron Microscope
SPPS	: Solid Phase Peptide Synthesis
TFA	: Trifluoroacetic acid
TEM	: Transmission Electron Microscope

CHAPTER 1

INTRODUCTION

1.1 Chemistry of Peptides

Peptides are a class of short polymers formed by the connection of amino acids covalently in which number of residues may possibly vary up to 100. They are also involved in some of the human biological processes in immune system¹ or in some others acting as enzymes² or hormones like insulin³ and glucagon.⁴ Other than that, they are capable of acting as neurotransmitters, neuromodulators as well as being involved in metabolism, pain, reproduction and immune response.⁵ In order to make all these applications well understood and develop, the first thing to be done is having a good command of chemistry behind the peptide research.

1.1.1 Definition and Structural Properties

In a more chemical way, peptides are oligomers (or polymers) in which the adjacent amino acids are connected to each other via an amide bond. This specific amide bond is also called as *peptide bond* and connects the carboxyl group of an amino acid with the amino group of the following one. As a worldwide accepted representation, the amino acid retaining its free amine group is written at left (called N-terminus) and the amino acid with the free carboxylic acid is written at right (called C-terminus).

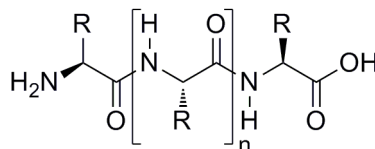


Figure 1.Chemical structure of peptides

In nature, 22 amino acids (including selenocysteine&pyrrolysine) are encoded by DNA. A collection of their names, structures and abbreviations is given in Appendix A. When the chemical structures of them are considered, each amino acid has a different side chain, generally represented as R group. These side chain groups contribute to the biochemical function of peptides and proteins.

The conformational flexibility of peptide chains is restricted to rotations around the bonds leading to the alpha-carbon atoms because of the rigidity of the amide bond. Having partial double bond character with a rotational barrier of approximately 65-90 kJ/mol forces the formation of two rotamers of the peptide bond.

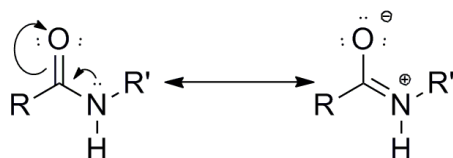


Figure 2.Resonance stabilization of the peptide bond

As it is shown in Figure 2, resonance stabilization of peptide bond is the factor that keeping the chain relatively planar and make it resistant to conformational changes. This structural feature may directly affect the conformations adopted by proteins and large peptides.

What about the distinction that makes one structure a hormone, another an antibody or structural protein? The answer to this question is exactly the difference in the chemical structures. According to their complexity, peptide and protein structures divided into 4 in a hierarchical way. Primary structures describe all the covalent bonds (mainly disulfide and peptide bonds) which link the amino acid residues in a polypeptide chain. Secondary structures refers to stable arrangement of a residue resulting with structural motifs and they are discussed in great detail in the following section. Tertiary structures stand for the 3D structural folding of peptides and protein subunits, and further arrangements of them results with quaternary structures.

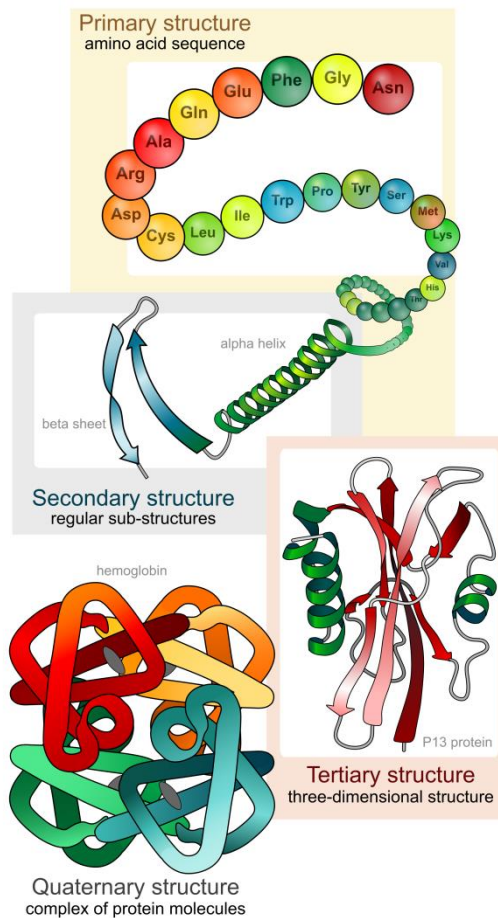


Figure 3.Peptide and protein structures in increasing order of their complexity.

1.1.2 Secondary Structures

As mentioned in the previous section, secondary structures express the ordered conformations of peptide backbone. This backbone conformation is characterized by backbone torsion angles ϕ and ψ of amino acid residues and dihedral angle ω of the peptide bond. The dihedral angle ω at the peptide bond is accepted as 180° for the reason that the partial double bond character creates relatively high rotational barrier and keep the peptide planar.

As it is seen in the figure below, in a polypeptide N-C $_{\alpha}$ and C $_{\alpha}$ -C bonds in the backbone are relatively free to rotate. These rotations are represented by the torsion angles phi (ϕ) and psi (ψ), respectively.

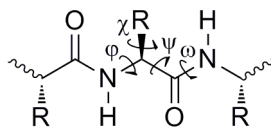


Figure 4. Torsion angles ϕ , ψ and ω .

When the steric interactions during rotation are taken into account, an overview of easily reached torsion angles can be obtained. These regions, eventually, are displayed in Ramachandran plot which was introduced by G.N. Ramachandran and his co-workers in 1963 in order to show the stereochemistry of polypeptide chain conformations.⁶ However, the actual conformation of a polypeptide under physiological conditions is determined by hydrogen bonds between peptide bonds, side-chain interactions, solvent effects and hydrophobic effects.

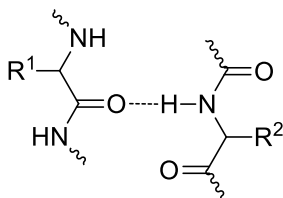


Figure 5. Typical hydrogen bond in peptides and proteins.

Hydrogen bonding patterns are main essentials in characterization of typical secondary structures in peptides and proteins. A hydrogen bond (Figure 5) chiefly is produced between the NH group (H-bond donor) and the carbonyl group oxygen (H-bond acceptor) of two interacting peptide bonds. The distance between the oxygen and nitrogen atoms considered necessary for the hydrogen bond generation is about 280 pm and the stabilization energy of a single hydrogen bond is relatively small ($20 \text{ kJ}\cdot\text{mol}^{-1}$) compared to a typical covalent bond ($200\text{--}400 \text{ kJ}\cdot\text{mol}^{-1}$). In most secondary structures that are stabilized by hydrogen bonding, more than a few hydrogen bonds are formed and these multiple interactions of such an accommodating system results with the stabilization of the whole secondary structure.

In this manner, the most important secondary structures are classified according to their torsion angle values. If the torsion angles of all amino acid residues in such an ordered structure have same values, then that structural element is considered as periodic. Helices and sheet structures are thought to be members of this group. On the other hand, if torsion angle values of amino acids in polypeptide chain are different, those secondary structures called as non-periodic which includes mostly turn structures. The figure below shows the representative images of these secondary structures.

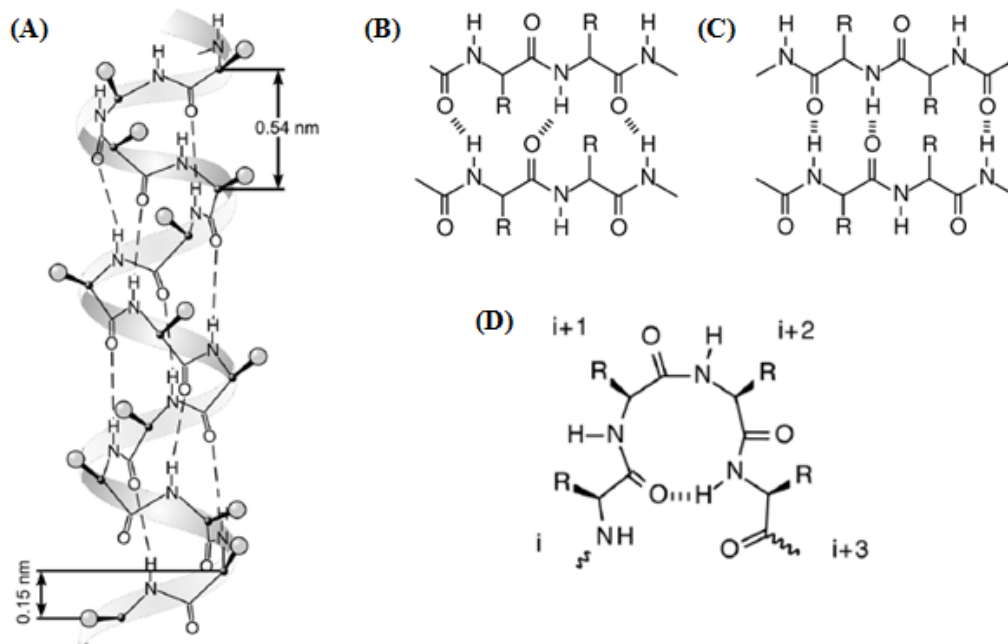


Figure 6. Peptide and protein secondary structures: A) α -helix, B) parallel β -sheets, C) antiparallel β -sheets and D) turn.

In addition to main secondary structural elements, there are few additional groupings named as supersecondary structures (or motifs) which occur mostly in globular proteins (Figure 7).

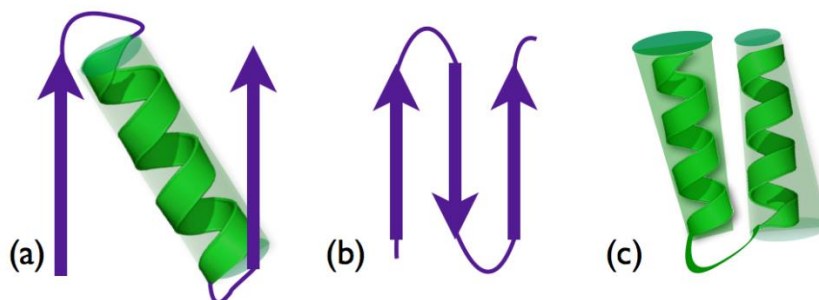


Figure 7. a) A $\beta\alpha\beta$ motif, b) a β hair pin motif and c) an $\alpha\alpha$ motif.

1.2 Peptide Hydrogels

Supramolecular hydrogels are a class of soft materials due to their wide range applications.⁷ For the development of these type of soft materials, molecular self-assembly dominates in preference which will be discussed in the following section. Hydrogels can be produced

from high molecular weight polymers (natural or synthetic), polysaccharides, proteins or relatively smaller synthetic organic molecules. Among all these hydrogelators, those made from amino acids, or more generally from peptides, attract great attention of scientists owing to their subsistent biodegradability and biocompatibility. The first examples of hydrogels from synthetic peptides were obtained serendipitously in the early 90's.⁸ Understanding of the molecular interactions and resulting secondary structures of peptides and proteins give researchers the chance for a rational approach to design and further develop the properties of these self-assembled materials. With this knowledge, applications of them can further be widened with some external stimuli. But before getting into detail about stimuli responsiveness, it is quite important to understand self-assembly phenomenon.

1.2.1 Self-Assembly

Self-assembly is a typical “bottom-up” process widely used in nanotechnology. It basically means the spontaneous association of molecules or ions to form larger and ordered structures through the formation of reversible interactions. The organization of the building blocks into ordered structures occurs when many different non-covalent interactions are combined. These interactions can be hydrogen bonds, electrostatic, hydrophobic or aromatic stacking interactions. Although these interactions are quite weak individually, the overall combination results with the formation pre-designed ordered structures which are both rigid and sophisticated.

The reversible nature of the self-assembly gives rise to a significant attribute of assembling systems which is the ability of them to correct ‘mistakes’ during the process and gradually work to form thermodynamically the most stable product. The reason for that is possibility of the existence of more than one combination. However, among all the combinations, one product of the assembly is going to be predominant due to higher thermodynamic stability over the others under the specific reaction conditions. Therefore, self-assembling systems can be considered as thermodynamically selective in product formation.

Although there many sub-classes of self-assembly, in many biological systems, the process can be aided by species that are not themselves incorporated into the final assembly which is called as ‘assisted self-assembly’. The process can be thought of as catalyzed self-assembly to compare with chemical catalysis is easy to make as the assisting species work by lowering the kinetic barriers for the formation of product.

As it is mentioned in the section 1.2, peptides have been recognized as very useful building blocks for creation of self-assembling materials. Especially β -sheet forming peptides demonstrate the extraordinary ability to assemble into 1D nanostructure for which the reason behind was explained in section 1.1.3. Consequently, further interactions among 1D nanostructures result with the formation of 3D networks.⁹

1.2.2 Formation of Structural Motifs in Peptides & Proteins

Molecular self-assembly is a powerful alternative to generate materials having wide variety of chemical and physical properties. In this boundless area, peptides are relatively promising for being building blocks. By combining 20 natural amino acids either with each other or with artificial ones, numerous types of materials with different properties can be produced. Despite the boundlessness of the subject, theoretical explanations of molecular interactions and self-assembly conditions have still been limited.

Among all the natural and synthetic peptides, a class of peptide, called “ionically complementary”, attains special interests because of leading to formation of complementary ionic pairs within each chain and/or between different chains. Ionic pairs in the same chain affect first of all the single-chain properties, but pairs between different chains help the stabilization of aggregates. Other than sharing some common properties with uncharged peptides (hydrophobicity and H-bonding), they own their unique charge properties that can distinctively control their aggregation behavior.¹⁰

Those mentioned charge properties are directly related to the pK values of the 20 standard α -amino acids which are tabulated in Table 1.

Table 1. pK values of 20 standard amino acids.

	Amino acid	α-carboxylic acid	α-amino	Side chain
1.	Alanine	2.35	9.87	
2.	Arginine	2.01	9.04	12.48
3.	Asparagine	2.02	8.80	
4.	Aspartic acid	2.10	9.82	3.86
5.	Cysteine	2.05	10.25	8.00
6.	Glutamic acid	2.10	9.47	4.07
7.	Glutamine	2.17	9.13	
8.	Glycine	2.35	9.78	
9.	Histidine	1.77	9.18	6.10
10.	Isoleucine	2.32	9.76	
11.	Leucine	2.33	9.74	
12.	Lysine	2.18	8.95	10.13
13.	Methionine	2.28	9.21	
14.	Phenylalanine	2.58	9.24	
15.	Proline	2.00	10.60	
16.	Serine	2.21	9.15	
17.	Threonine	2.09	9.10	
18.	Tryptophan	2.38	9.39	
19.	Tyrosine	2.20	9.11	10.07
20.	Valine	2.29	9.72	

As it is seen in the table, pK values of the α -carboxylic acid groups lie in a small range near 2.2 which means above pH 3.5, these groups are almost entirely in their carboxylate forms. On the other hand, the α -amino groups all have pK values around 9.4 and are almost entirely in their ammonium ion forms below pH 8.0. These leads and important structural feature: *In the physiological pH range, both the carboxylic acid and the amino groups of α -amino acids are completely ionized.* Therefore, amino acids form zwitter ions (bearing charged groups of opposite polarity) in neutral pH (Figure 8).

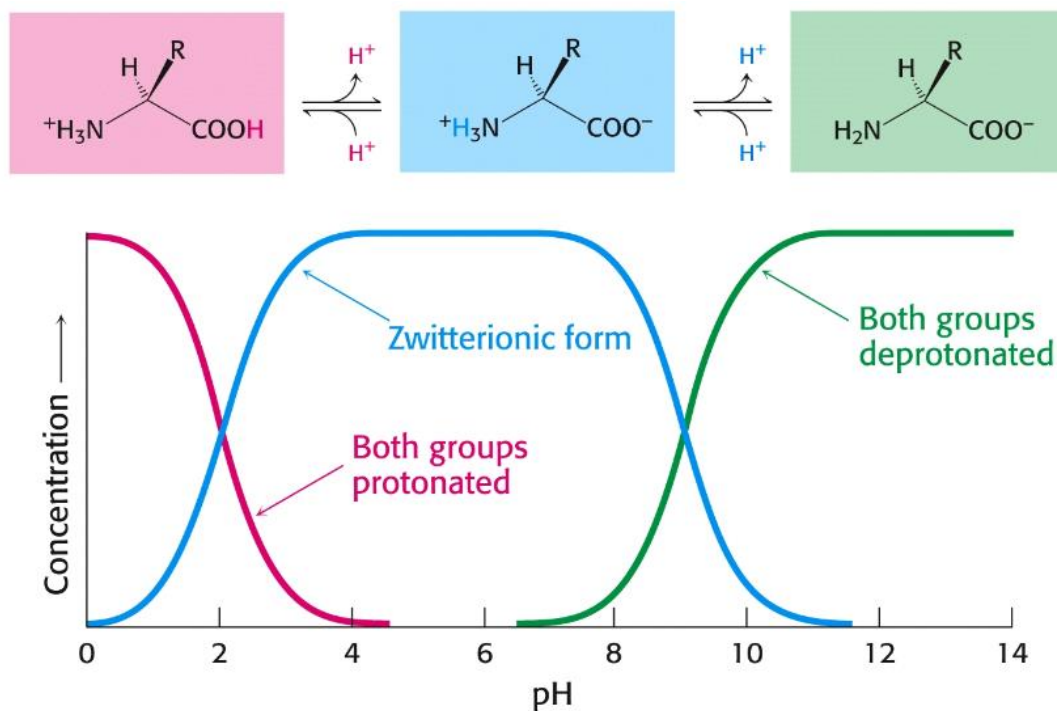


Figure 8. Ionization state of amino acids.

After 11 years from the discovery of one of these peptides (EAK16-II), by Zhang and his co-workers¹¹, Jun et al. (2004), reported the effect of charge distributions on self-assembly with detailed theoretical and experimental studies⁴. In that study, they showed basically that, single molecule properties highly effective on the self-assembly of charged oligopeptides (Table 1).

Table 2. Results of charge distribution in a peptide with same amino acid recipe.

Name	Sequence	Charge Distribution	AFM Results	FT-IR Results
EAK16-I	AEAKAEAKAEAKAEAK	-+--+--+--+	Fibrillar Nanostructures	β -sheets
EAK16-II	AEAEAKAKAEAEAKAK	--++--++	Fibrillar Nanostructures	β -sheets
EAK16-IV	AEAEAEAEAKAKAKAK	-----++++	Globular Nanostructures	Turns (from bending of molecules)

In addition to effect of charge distribution, there are some other factors that influence degree of self-assembly. One of them is hydrophobicity, that can be narrowed down as the interaction between aromatic units and it highly affects molecular recognition and self-assembly processes. There are several theoretical and experimental findings pointing out the formation of high-order clusters from aromatic rings.¹² To be more specific, one can say that aromatic side-chain interactions play a central role in self-assembly of peptides, but that contention has still been a controversial issue. Bowerman *et al.* showed in their study that aromatic interactions are not strictly required for self-assembly. By choosing amphipathic (FKFE)₂ peptide as a model system, they conducted secondary structure analyses with peptides derived from the model (Table 3).

Table 3. (XKXE)₂ peptide sequences, hydrophobicity, and secondary structure propensity. (^a Amino acid hydrophobicity based on water-octanol partition coefficients relative to Gly. ^b Propensity to occur in β -Sheet secondary structures.)

Peptide	Sequence	X	Π^a	β -Sheet Propensity (P_β) ^b
1	Ac-(FKFE) ₂ -NH ₂	Phe	1.79	1.33
2	Ac-(AKAE) ₂ -NH ₂	Ala	0.31	0.75
3	Ac-(VKVE) ₂ -NH ₂	Val	1.22	1.86
4	Ac-(LKLE) ₂ -NH ₂	Leu	1.70	1.1
5	Ac-(ChaKChaE) ₂ -NH ₂	Cha	2.72	-

Upon the light of CD, AFM and TEM analyses, it can be said that when the aromatic phenyl alanine residues are replaced with nonaromatic natural ones having lower hydrophobicity (Ala, Val and Leu) and nonnatural cyclohexylalanine (Cha), aromatic interactions may not be strictly required for amyloid formation and that nonaromatic by highly hydrophobic structures can have unique characteristics in self-assembly and enhanced hydrogelation properties.¹³

Although much more extended studies must be conducted, even a single model peptide can give detailed information about potential structural motifs depending on every single factor affecting self-assembly.

1.2.3 Stimuli Responsive Peptide Hydrogels

In particular, peptide based hydrogels are very important functional material owing to their biocompatibility with wide range applications.¹⁴ But one thing to remember is the control of self-assembly process which is a significant challenge in molecular self-assembly and avoiding defects in the assembled structures. Because many of the systems, both single and multi-component, face the problem that when the material is once put into water or buffer, self-assembly is immediately starts, therefore nucleation and growth steps are inadequately controlled. For that reason there is an increasing focus on development of systems that can assemble and disassemble by responding some external stimuli.

Stimuli that have been used to trigger hydrogelation of peptides include a variety of chemical and physical means, such as changes in ionic strength, pH, temperature, light, addition of some chemical entities, formation of certain chemical bond, and enzymatic transformations.² Among all these factors, pH changes are often consequences of protonation or deprotonation of basic and acidic amino acids (see Appendix A). Or since peptide folding is sensitive to temperature changes, temperature is often employed to trigger a change in peptide conformation. Increasing the temperature is often leads to unfolding of the secondary structure and thus disruption of function is occurred. Besides, heat-induced denaturation can also give us detailed information about the thermodynamic stability of proteins. Additionally, enzymes have important roles in cell pathways and disease states including the synthesis and assembly of structural protein scaffolds which can also be used in enzymatically switched materials.¹⁵ Lastly, among the choices of external stimuli, light is an appropriate candidate for the modulation of hydrogels' condition because it acts in non-contact and site-specific fashion and delivers relatively easy and precise control of irradiation conditions.

1.2.4 Examples for Stimuli Driven Peptide Hydrogels

Among the triggers for hydrogelation, disulfide bond formation is a useful technique to prepare bioconjugates in which two structurally different entities are joined together to construct conjugated larger molecules. Nilsson and Bowerman (2010) used this strategy to remove the conformational constraints in a cyclic peptide with the reduction of disulfide bond which is quite important in biologically relevant microenvironments and it is stated that development of reductive trigger for stimuli responsiveness has considerable potential for application in biotechnology.¹⁶

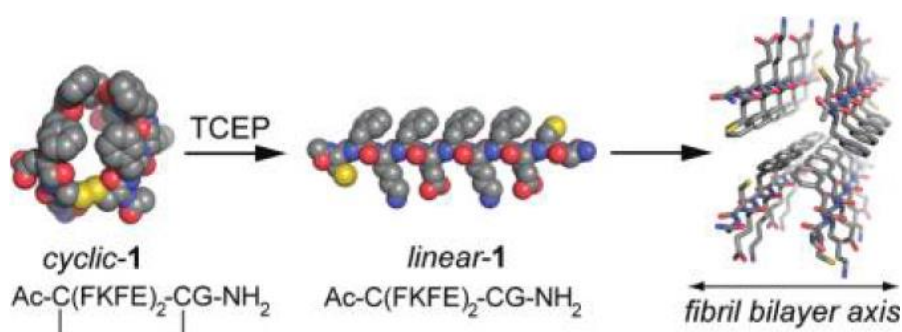


Figure 9. Schematic representation of the cyclic to linear peptide conformational switch using a reductive trigger.

The flanking cysteine residue of a self-assembling amphipathic peptide sequence Ac-(FKFE)₂-NH₂ was reported to be cyclized via disulfide bond formation which imposes a conformational limit (Figure 8). That steric constrain prevents the peptide from forming the β -sheet conformation which is crucial for self-assembly to occur. When the disulfide bond is reduced, peptide relaxes and forms the desired β -sheet conformation and further self-assembles into a fibrillar structure (Figure 9).

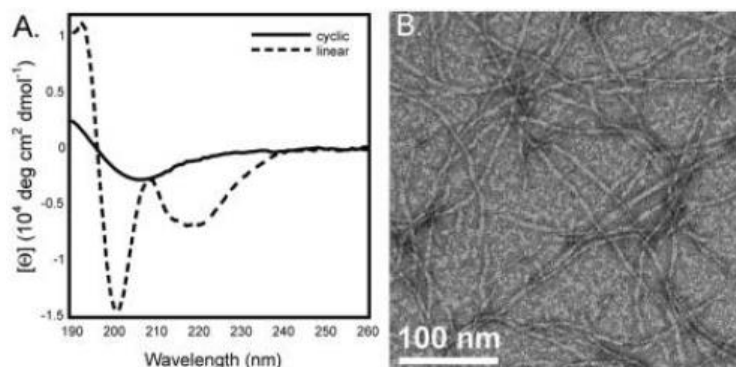


Figure 10. a) CD spectra of cyclized and reduced (linear) form of peptide. (b) TEM image of fibrillar linear peptide.

On the other hand, complexation of metal ions by peptides also attract particular interest for which the formation of structurally defined materials. Nature includes also some interactions of metals with histidine, methionine, cysteine, aspartic acid and glutamic acid residues which induce conformational changes in proteins to force diverse biological reactions in addition to formation of supramolecular structures. Especially zinc ion is a cofactor for enzymes involved in cell replication, protein synthesis etc. Schneider et al. worked with a 20 residue β -hairpin peptide (Figure 10) where a negatively charged non-natural amino acid residue is incorporated to the backbone in order to promote metal ion binding property.¹⁷

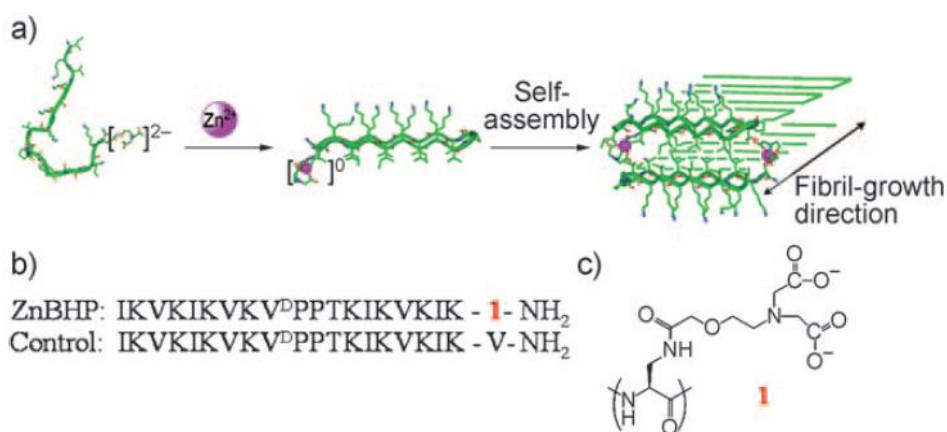


Figure 11. a) Proposed mechanism of metal-triggered folding and self-assembly. b) Primary sequences of Zn-beta hairpin peptide and the control peptide. c) Structure of the non-natural amino acid **1** (3-amidoethoxyaminodiacetoxy-2-aminopropionic acid).

While the peptide stays as unfolded and soluble in water, it undergoes folding and further self-assembly forming a β -sheet involving fibrillar hydrogel which having relatively rigid viscoelastic properties. Additionally, they reported that all the CD, FTIR and mass spectroscopic measurement confirmed a 1:1 binding of the peptide and Zn^{2+} in hydrogel formed in presence of that metal ion.⁸

Although there are a variety of choices for external stimuli, light is a very suitable candidate for modulation of the state of hydrogel because it acts externally and site-specifically and these features provide easy and precise control of irradiation and further hydrogelation. Schneider et al. reported in their another study a photochemical approach relies on the photocaging of the amino-acid side chain functionality. For that purpose, they employed a α -carboxy-2-nitrobenzyl cage in the β -hairpin peptide hydrogelator series to MAX7CNB (Figure 11).

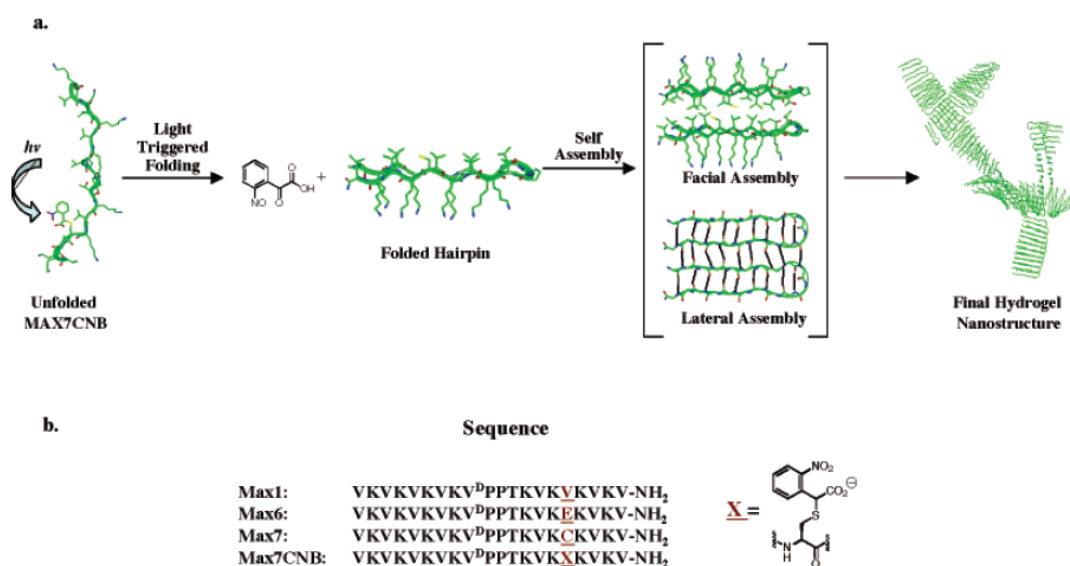


Figure 12.(a) Light induced material formation. (b) Sequences of carboxyamidated peptides.

The sequence MAX7CNB remains unfolded and unable to assemble when it is dissolved in aqueous medium. However, irradiation of the solution (260 λ 360 nm) releases the photocage and triggers peptide folding to produce amphiphilic β -hairpins which self-assemble into viscoelastic hydrogel material.¹⁸

1.3 Solid Phase Peptide Synthesis (SPPS)

The concept of peptide synthesis on a solid support was first developed by Robert Bruce Merrifield¹⁹ in 1963. It is based on the idea that a peptide chain can be assembled in a stepwise manner while it is attached at one end to a solid support. Today, the concept has been extended not only to peptides but has been used in organic synthesis on polymeric supports as well.

In standard Merrifield's method, protecting groups based mainly on benzyl and t-butyl derivatives (especially Boc) are used. The *tert*-butyloxycarbonyl group is used for temporary N α -protection which requires selective cleavage at every cycle of amino acid addition. Usually, Boc is cleaved with TFA (20-50 %). However, with this temporary protecting group, the more permanent benzyl derivatives that used for side chain and C-terminus protection (peptide-resin linkers) are acid labile. Therefore, loss of some portion of side chain protectors and of the peptide-resin linkers occur at every cycle and this feature makes the absolute selective cleavage impossible and also lowers the final yield.

On the other hand, the Fmoc-protecting group tactics provide base labile cleavage. Although introduced into peptide chemistry in 1970, the Fmoc/Boc method has been used in SPPS

only since 1978. With its two dimensional orthogonality, Fmoc/Boc method is a widely preferred alternative to Boc/Bzl scheme. Fmoc can be cleaved by base-catalyzed elimination in which the secondary amine (Piperidine) also traps the dibenzofulvene formed in the reaction. After the peptide chain growth is completed, acid labile peptide-resin linkers and mostly Boc type side chain protecting groups can be cleaved at the same time under mild reaction conditions with TFA.

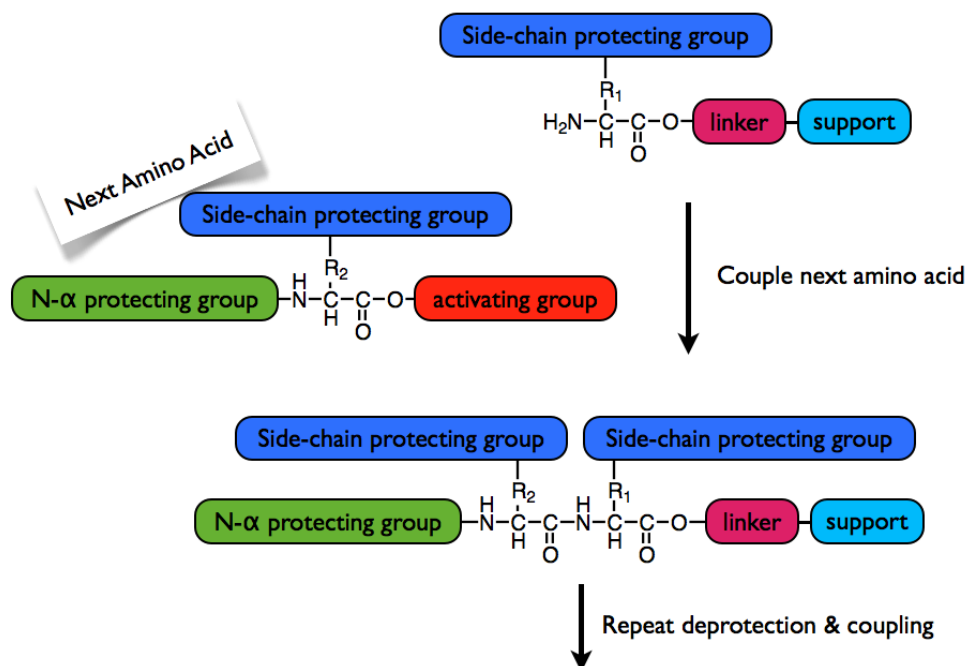


Figure 13. Schematic representation of solid phase peptide synthesis employed with Fmoc chemistry.

1.3.1 Advantages over solution based methods

Solid phase peptide synthesis provides significant advantages over classical solution phase method. First of all, since the peptide is synthesized while its C-terminus is attached covalently to an inert polymeric support, there is no need to perform time-consuming isolation and purification of all intermediates which is needed in solution phase synthesis. Hence, the product of all reactions for peptide chain growth remains bound to resin and excess reagents are removed together with by-products by filtration. During the course of synthesis, no mechanical loss occurs because the growing chain is retained on the polymeric resin in a single reaction vessel. At the end, the final peptide is cleaved from the resin by a single cleavage step. In this step, the side chain protecting groups can also be cleaved which makes the final work-up and isolation much easier.

With all these simple technical operation and potential automation, solid phase synthesis provides an effective solution for scientists in chemical synthesis of polypeptides and

proteins. At this point, it can easily be said that Merrifield synthesis is a major impact on chemical peptide and protein synthesis as well as on solid phase organic synthesis. For this unique invention which has revolutionized organic chemistry, Merrifield was awarded the Nobel prize in 1984. Today, the concept has already been generalized to organic synthesis on polymeric supports, which includes both heterogeneous reactions involving insoluble polymer and homogeneous reactions like liquid phase peptide synthesis with soluble polymeric material.

1.3.2 Reactions & Mechanisms

In SPPS, Fmoc/Boc approach, the C-terminus of residue is attached to a TFA-labile linker and the functional groups on side chains are protected with TFA-labile linkage agents as well. The temporary N-Fmoc protecting groups can be removed with 20 % (v/v) Piperidine in DMF. The deprotection mechanism is shown in Figure 13. Initial deprotonation of the fluorenyl ring is the key step to produce aromatic cyclopentadiene type intermediate. It rapidly eliminates to form dibenzofulvene which is then scavenged by piperidine. The product of deprotection has a distinctive UV absorbance so that reaction can be monitored by this way.

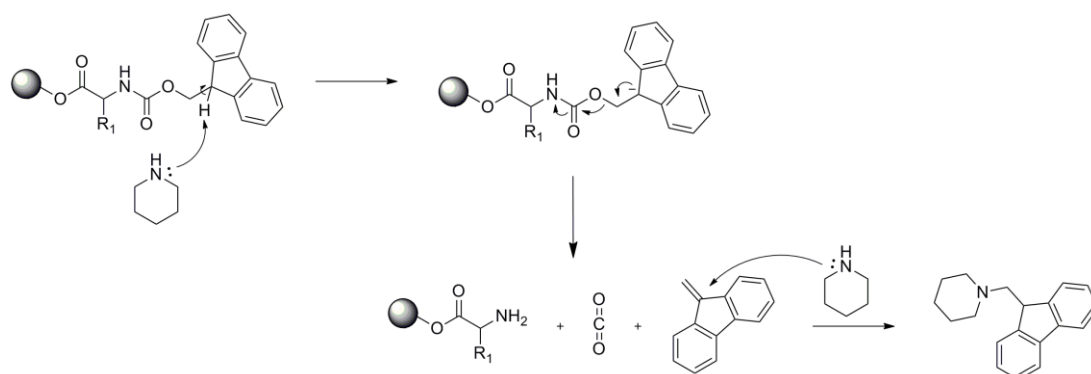


Figure 14.N-FmocDeprotection mechanism.

Following the deprotection step, the stepwise introduction of N α -protected aminoacids is composed of in situ carboxy activation of the incoming aminoacid. So, coupling is generally carried out in DMF or NMP with the usage of activation agents. In order to drive the acylation to completion an excess of activated amino acid is used, usually the 2– 6 times the resin functionality. HBTU included activation is shown in Figure 14.

On the other hand, there is one important consideration in coupling step which is maintaining the effective concentration of reagents as high as possible. Therefore, in small scale synthesis, in our study as well, with resins having low substitution values, large excess (4-5.5 fold) of reagents are needed.

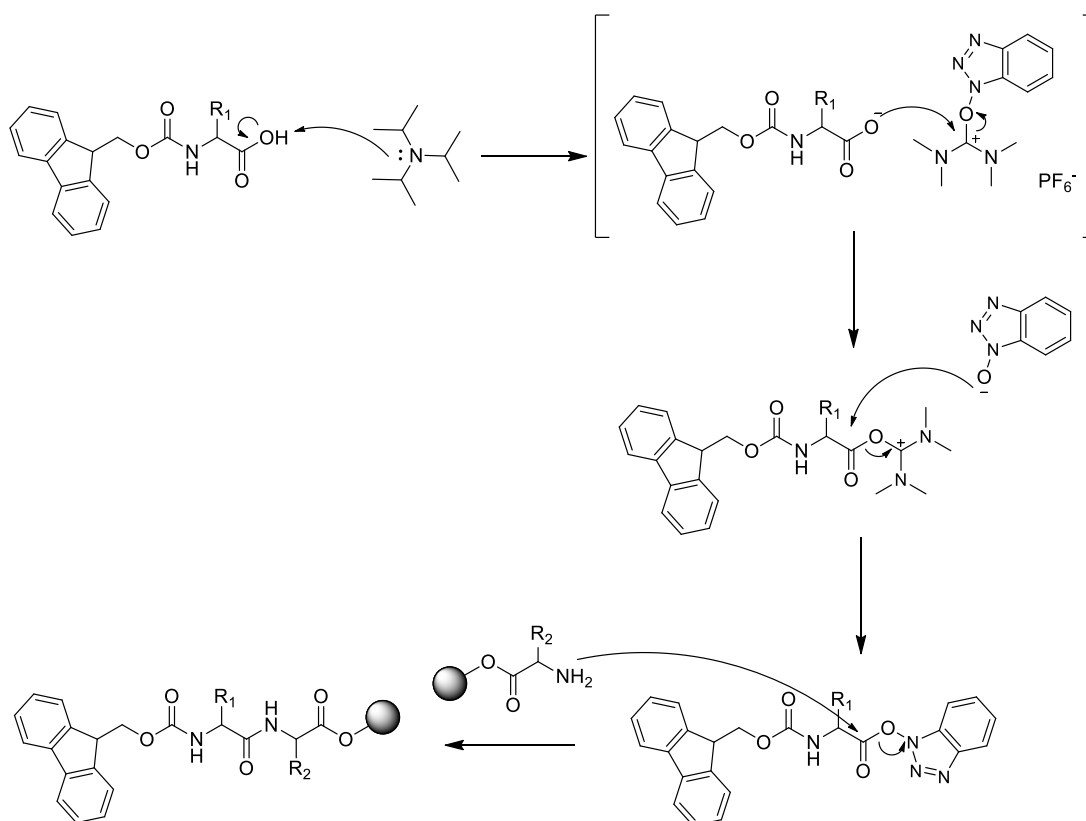


Figure 15.C-terminus activation via HBTU-DIEA mechanism.

1.4 Photochemistry of Azobenzene

Although the first azo-dye was discovered by Martius in 1863, it is reported that the fully elucidated photochemical reaction of azobenzene was first reported by Krollpfeiffer and his coworkers in 1934. Just after 3 years of his achievement, a further important discovery was made by Hartley who observed the photochemical *cis/trans* isomerization of azobenzene for the first time, will be explained in the following section. After his cornerstone observation, azobenzene photochemistry has been huge attention by scientists.²⁰The term photochemistry actually includes a few branches but in the following section photochemical *cis/trans* isomerization will be focused. But before that, knowledge of the excited states and light absorption is essential in order to understand its photochemical reactions.

1.4.1 Electronic Absorption Spectra and Excited States

The two isomeric compounds (*E*) and (*Z*) azobenzene (IUPAC name: 1,2-diphenyldiazine) possess $2 \times 6\pi$ electrons in the two phenyl rings, 2π electrons in the azo group and 2 electrons

in each lone pair of the two N-atoms. Therefore, it can be expected various $n \rightarrow \pi^*$ and $\pi \rightarrow \pi^*$ transitions to take place.

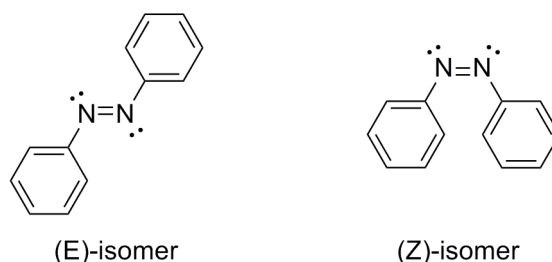


Figure 16. (E) and (Z) isomers of azobenzene.

The light absorption properties of cis- and trans- azobenzene have been calculated by MO with varying methods and it has been found that the results correlate with the related experiments^{21,22,23} (Figure 16).

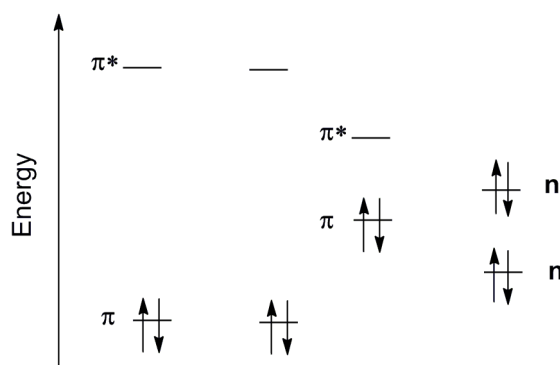


Figure 17. Schematic MO diagram for Azobenzene.

From left to right, the relative energy levels of the three highest occupied (HOMO) and the three lowest unoccupied (LUMO) π orbitals are shown which are followed by the occupied non-bonding n orbitals of nitrogen ion pairs. In the absorption spectra of (E) and (Z) azobenzene ;

- $n \rightarrow \pi^*$ transition appears as a weak band at $\lambda = 450\text{nm}$ ((E), $\epsilon = 463 \text{ M}^{-1} \text{ cm}^{-1}$)
 $\lambda = 430\text{nm}$ ((Z), $\epsilon \approx 1500 \text{ M}^{-1} \text{ cm}^{-1}$)
- $\pi \rightarrow \pi^*$ transitions cause strong second bands at $\lambda = 330\text{nm}$ ((E), $\epsilon \approx 17000 \text{ M}^{-1} \text{ cm}^{-1}$)
 $\lambda = 280\text{nm}$ ((Z), $\epsilon \approx 5100 \text{ M}^{-1} \text{ cm}^{-1}$)

Since (Z)-azobenzene is non-planar for stereoelectronic reasons, some mixing of n and π orbitals occur and this explains the higher intensity of the corresponding $n \rightarrow \pi^*$ and the weaker $\pi \rightarrow \pi^*$ absorption.²⁴

1.4.2 Cis/Trans Isomerization

Azobenzene undergoes cis/trans isomerization with absorption of two different wavelengths of light. In each case, the incident photon promotes an electron to a π^* orbital. First accessible excited state has $n\pi^*$ character and the second one has $\pi\pi^*$ for the reason explained in the previous section. Both transitions are focused on the N=N bond and resulting with a reduction of π bond.

However, behind the consequence of the isomerization, its detailed mechanism has still been a controversial subject. Although some of the previous experimental studies²⁵ suggested the inversion mechanism, some researchers suggested rotation mechanism and some suggesting a competition between them.²⁶

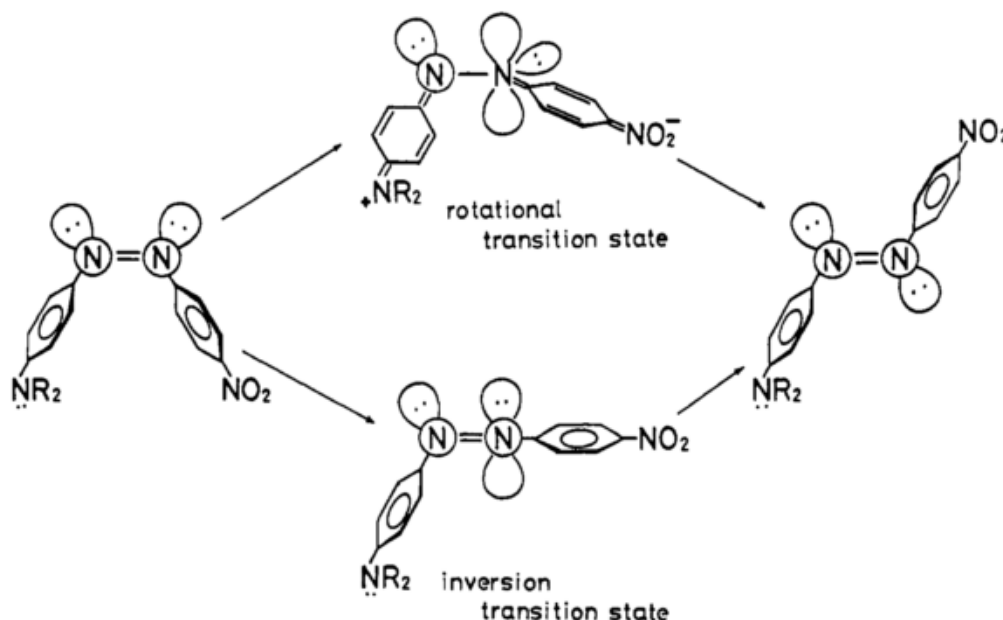


Figure 18. Proposed Mechanisms for Cis/Trans isomerization of azobenzene.

Despite the studies about mechanism of isomerization has still been continuing, a more recent study includes comparison of azobenzene structural dynamics under laser irradiation and/or external mechanical loads. Under those circumstances, it is stated that the photoisomerization of azobenzene is largely an excited-state dynamics through the rotation of C-N-N-C dihedral torsion angle instead of the inversion of the C-N-N in-plane bending angle.²⁷

1.4.3 Azobenzenephotoswitches

Azobenzene has been known for a century with its photochromic properties as well as the ability to isomerize very easily. Hence, photoswitching properties of azobenzene have been studied extensively by scientists. These photoswitching properties have been used in wide variety of biomolecules including peptides, proteins, nucleic acids, oligonucleotides, lipids and carbohydrates.²⁸

For the photo-control of peptides, significant investigations have been made for azobenzene-mediated photo-control of structure and functions. In 2011, Huang and co-workers reported that short peptides were found to be motif and pH dependantsupramolecularhydrogelators when they are properly linked with azobenzene as conformational switch element.²⁹ They found that amino acids with aromatic side chains like Phe and Tyr are highly favorable for short peptides to form hydrogels at suitable pH. On the other hand, cationic amino acid residues such as Arg and Lys were found to effect hydrogelation negatively. While studying hydrogelation properties of a series of short peptides, it was also realized that some of them had photoresponsive properties with E-/Z- transition upon light irradiation.

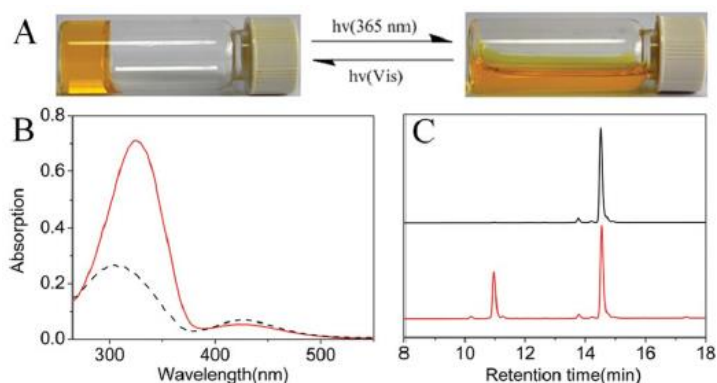


Figure 19. a) Optical images of photo-induced phase change of hydrogels formed by azo-Gln-Phe-Ala. b) UV-spectrum of the same hydrogel, before (red solid line) and after (black dash line) UV irradiation. c) HPLC monitoring of the hydrogel, before (upper) and after (lower) photo-induced phase change.

By trapping vitamin B12 in the hydrogel, it has also been shown that azo-Gln-Phe-Ala accelerated the release process upon photo-irradiation compared to diffusion controlled release which also demonstrates that azobenzene included photoswitches can effectively be used for drug delivering systems.

Additionally, photochromic azobenzene linker can be incorporated as turn element into the peptide backbone. Aemissegger et al. reported a β -hairpin forming peptide in which azobenzene acts as turn element.³⁰ Backbone incorporation of azobenzene resulted with oligomer formation when the azo-linker in its thermodynamically favored trans form. On the other hand, light-triggered conformational change of the linker to its cis form led to the

formation of monomers having β -hairpin structure for which determination was achieved with $^1\text{H-NMR}$.

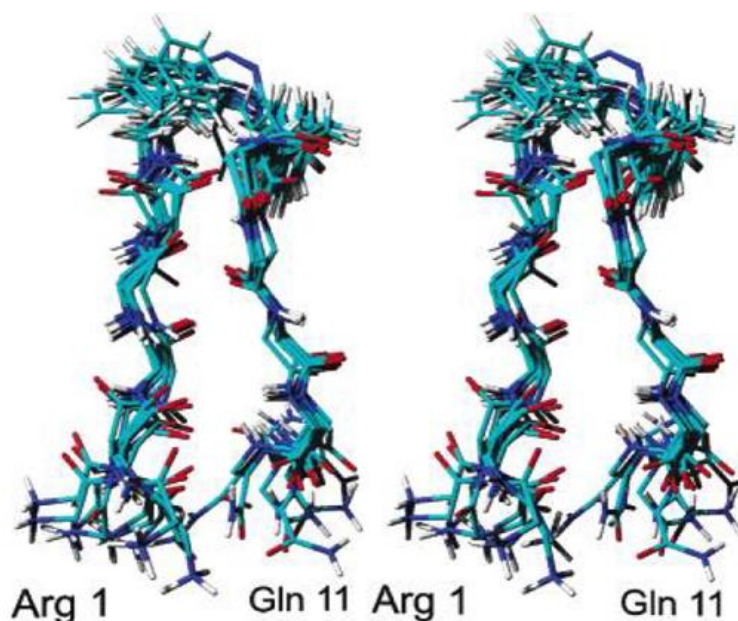


Figure 20. Cross-eyed superposition of the 10 best structures of the azobenzene containing peptide derived from GB1 protein.

With the amino acid sequence known to fold into β -hairpin structure in aqueous solution, a total of 100 structures were determined from the NMR data. As it is shown in Figure 19, the superposition of the best 10 structures indicates that the peptide can form a hairpin structure having considerable flexibility both at termini and also in the turn region. All those results suggested that properly substituted azobenzenes have great potential for being photoinducible turn elements and can be used to control the folding and stability of β -sheet and β -hairpin structures.

1.5 Aim of the Study

The main objective of this project is to achieve light controlled self-assembly and hydrogelation of pre-designed peptides. For that purpose, azobenzene containing artificial amino acids are incorporated to peptide backbone to control conformation of peptides with light. For the synthesis of peptides certain natural amino acids are preferred to produce special secondary structures. Although trans azobenzene is more stable than its cis form, when the system is irradiated with light, peptides are aimed to be transformed from trans to cis conformation. With this transformation peptides are going to be able to form β -hairpin structure which is the key factor for generating strong self-assembly and further hydrogelation (Figure 21).

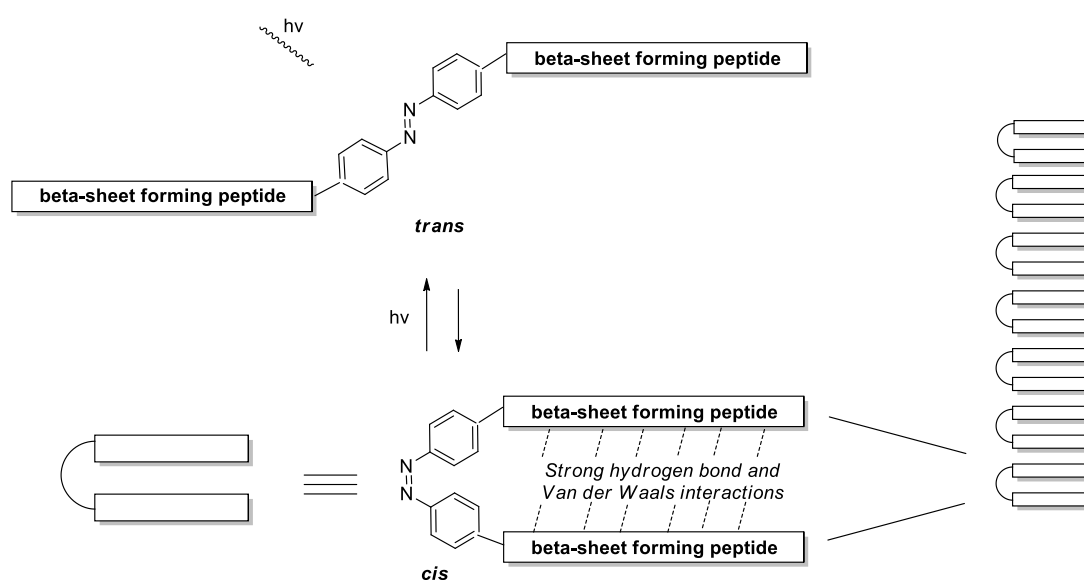


Figure 21. Schematic diagram of photochemical isomerization of azobenzene containing peptides.

With the unique design of the system, reversible cis-to-trans isomerization can be achieved and disruption of the hydrogel can be used as a selective drug delivery system.

CHAPTER 2

RESULTS AND DISCUSSION

Up to now, there have been many peptide sequences reported that are capable of forming β -sheet structures. These peptides are mostly consisting of alternating charged amino acids and it is mostly stated that ionic complementarity is the key factor in these types of peptides.

In this study, peptides are designed in such a way that each sequence contains hydrophilic glutamic acid (E) and lysine (K) for providing charge alternation and hydrophobic phenyl alanine (F) or alanine (A). Each single parameter may have significant effects on hydrogel formation such as peptide concentration, pH, type and time of photoirradiation. Therefore we examined only couple of them and in each step we tried to change only single parameter which mostly based on the structure of peptides.

For the light responsiveness, two different amino acids were synthesized³² in which azobenzene is preferred for its easy cis/trans isomerization (Figure 21).

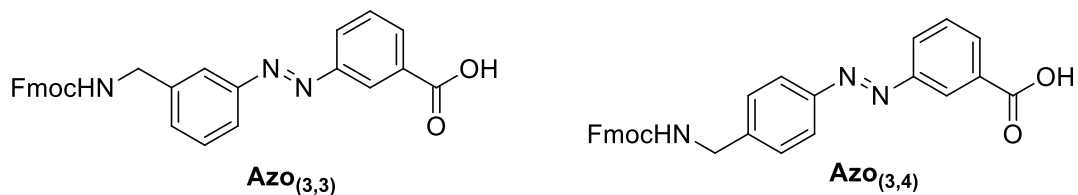


Figure 22. Structures of azobenzene containing artificial amino acids.

The importance for the preference of azobenzene is highly associated with its geometrical change while the isomerization proceeds. The conversion of trans-isomer to cis- results with the reduction of distance between 4 and 4' ring positions from 9.0 to 5.5 Å.³¹ On the other hand, this distance gets smaller for Azo_(3,4) and even more for Azo_(3,3) artificial amino acids incorporated peptides.

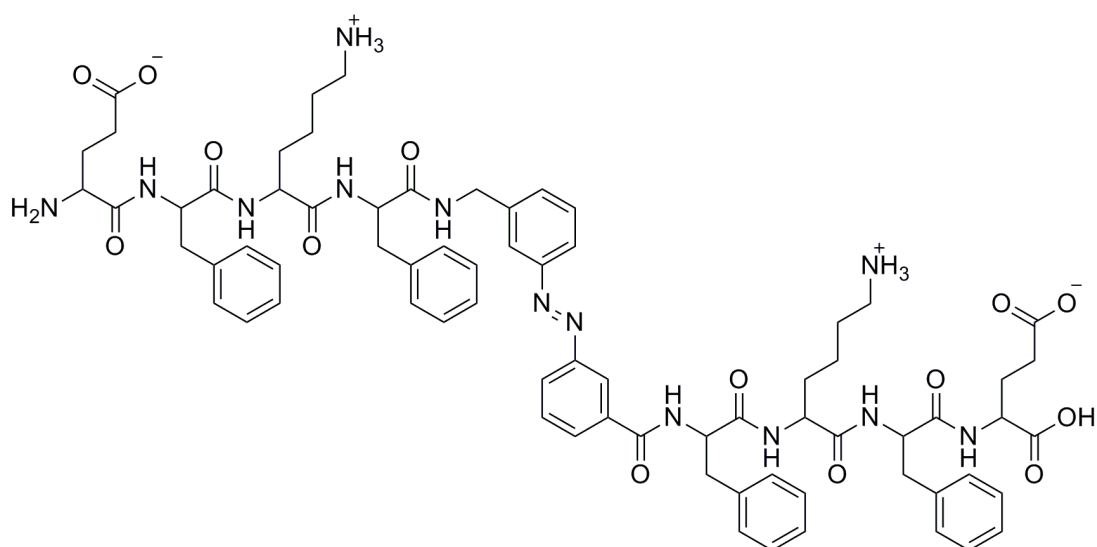


Figure 23. Structure of *Peptide 1* with sequence EFKF-Azo_(3,3)-FKFE.

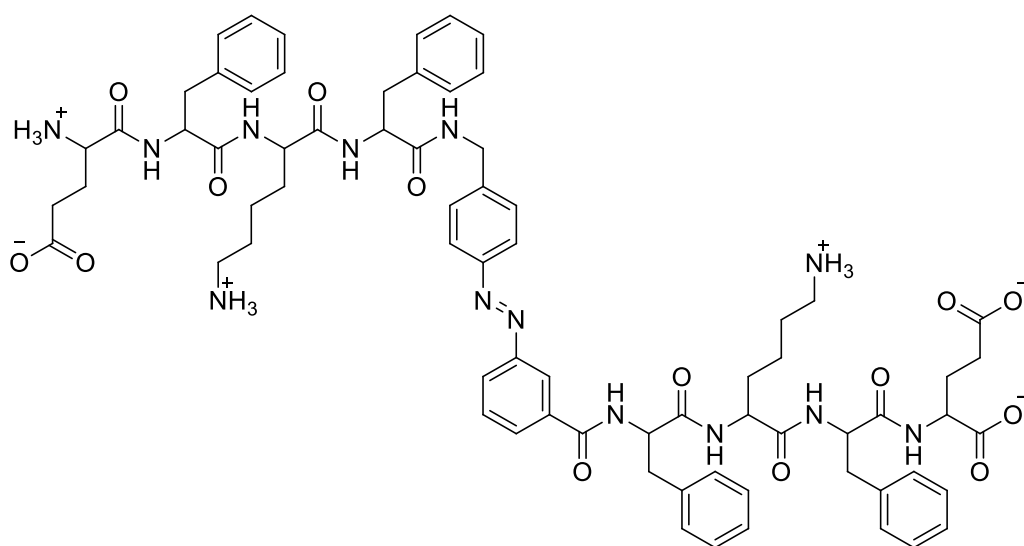


Figure 24. Structure of *Peptide 2* with sequence EFKF-Azo_(3,4)-FKFE.

Therefore we first synthesized *Peptide 1* and *Peptide 2* with 0.1 mmol scale with Solid Phase Peptide Synthesis (SPPS) method and investigated the effect of distance between the peptide chains on each side of the azobenzene (Figure 22& 23). In the purification and further characterization of these peptides, one point needs to be paid attention. Although trans isomer is much more stable than its cis form, two different peaks have always appeared in HPLC spectra of purified peptides (See Appendix C) which was first considered as impurity (Figure 24). However, absence of the former peak in the HPLC spectrum at 330 nm

wavelength makes us presuming that two isomers of the azobenzene bearing peptides might have been situated in the same matrix.

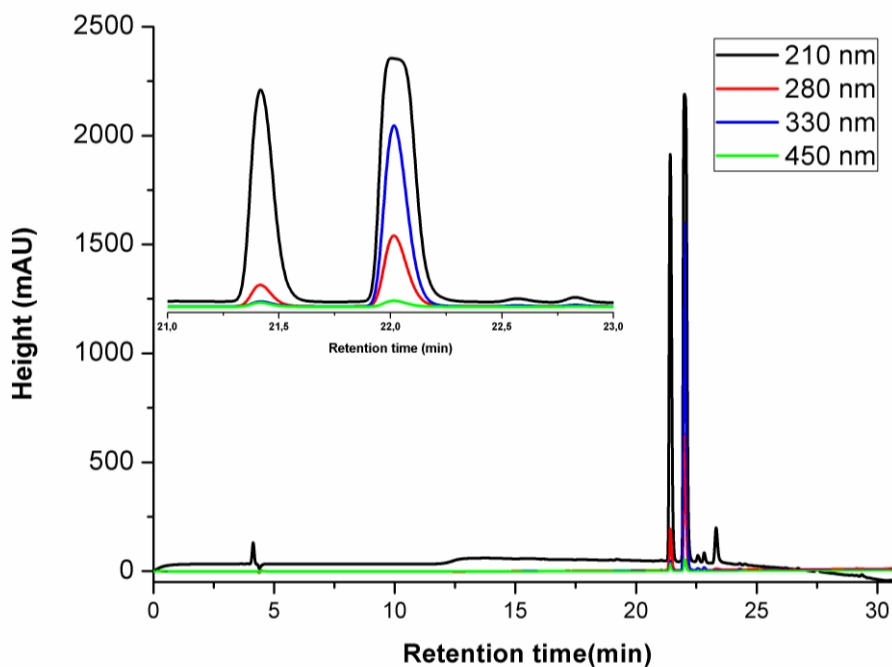


Figure 25.HPLC chromatogram of azobenzene containing *peptide 1*.

Our assumption is confirmed by LC-MS measurements which show that these two peaks have identical mass spectrum (See Appendix B). This result is quite unusual because without irradiation of trans isomer, cis isomer does not usually exist and in general cis isomer is not stable for a long time and slowly converted into trans isomer. This might show that cis isomer is stabilized by the formation of hairpin structure which supports the aim of this project.

Gelation studies were conducted in which during the photoirradiation CD measurements were carried out in every hour and over 12 hour to see change in β -sheet character of 9mM peptide solutions. Analysis between 190 and 260 nm gives information about the secondary structure contents. Especially for peptides and proteins, positive and negative bands at around 200nm indicate β -sheet or random coil formation.³²

First of all, in order to see 3D depth profile of peptides in nanoscale, SEM images of *Peptide 2* were taken (Figure 27). However, in our study, focusing on much smaller scales is more important that is why we have continued our nanostructure investigations only with TEM analysis. Since it is expected to see some more rigid nanostructures (like intertwined fibril formations) TEM images of peptides before and after UV irradiation were compared.

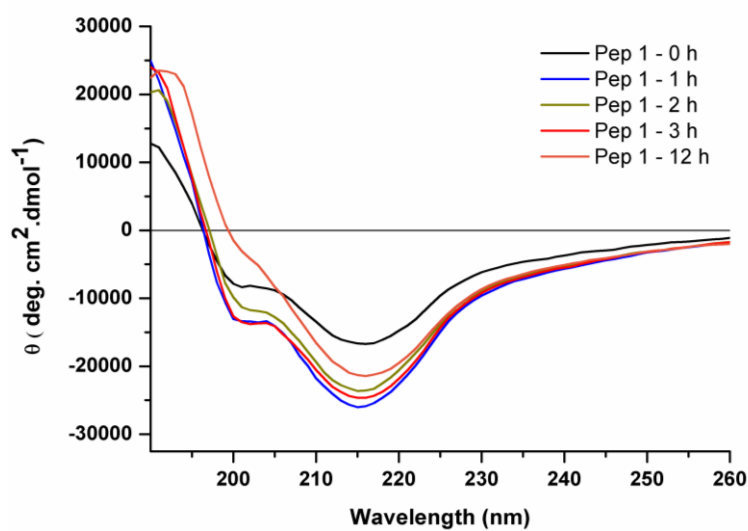


Figure 26.CD Spectrum of *Peptide 1*.

As it is seen in Figure 26, β -sheet character of the system increased starting from the beginning of photoirradiation. In Circular Dichroism, $n \rightarrow \pi^*$ transition is primarily responsible for the negative bands at 216-218 nm and $\pi \rightarrow \pi^*$ transition is responsible for the positive band at ~ 198 nm which are the characteristics of β -sheet spectrum.

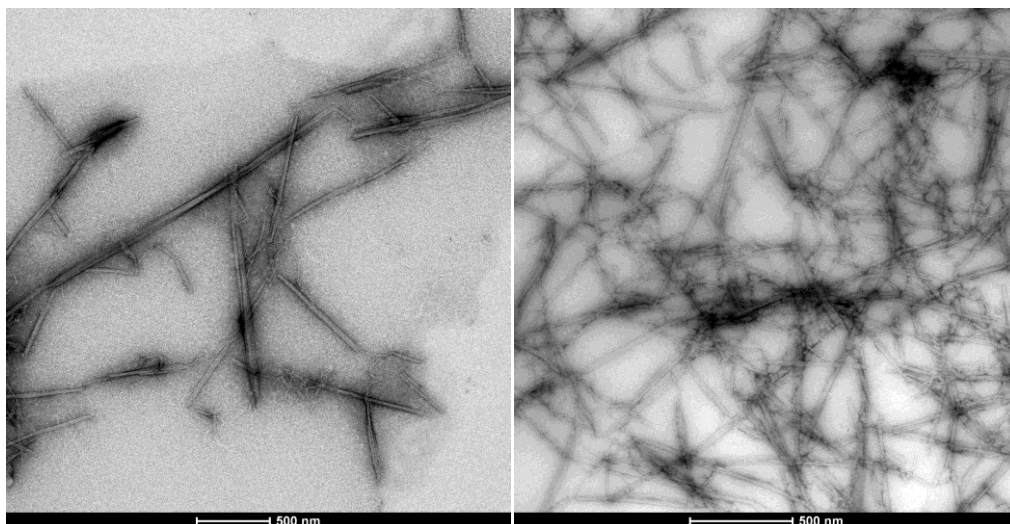


Figure 27.TEM images of *Peptide 1* : EFKF-Azo_(3,3)-FKFE.(Before UV on the left and after UV on the right side).

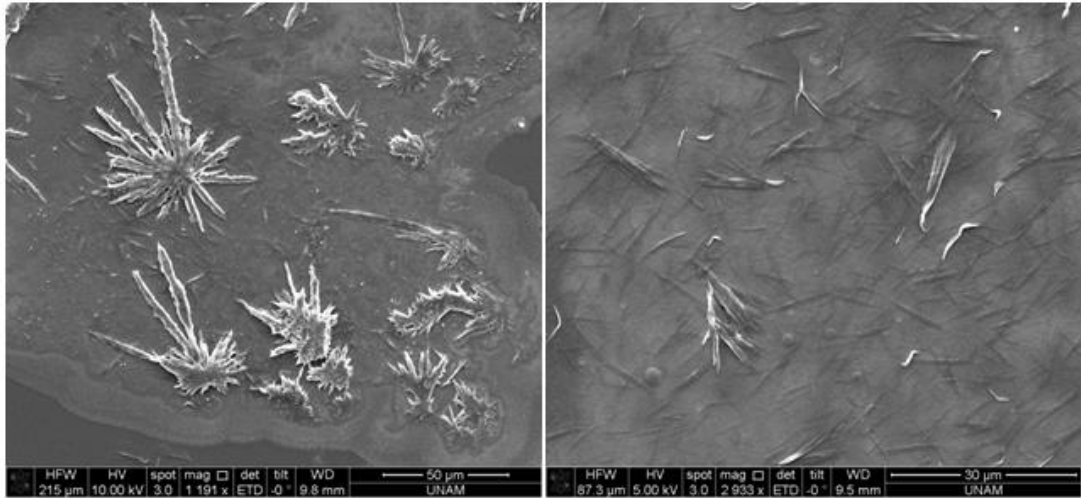


Figure 28. SEM images of *Peptide 2* : EFKF-Azo_(3,4)-FKFE (Before UV on the left and after UV on the right side).

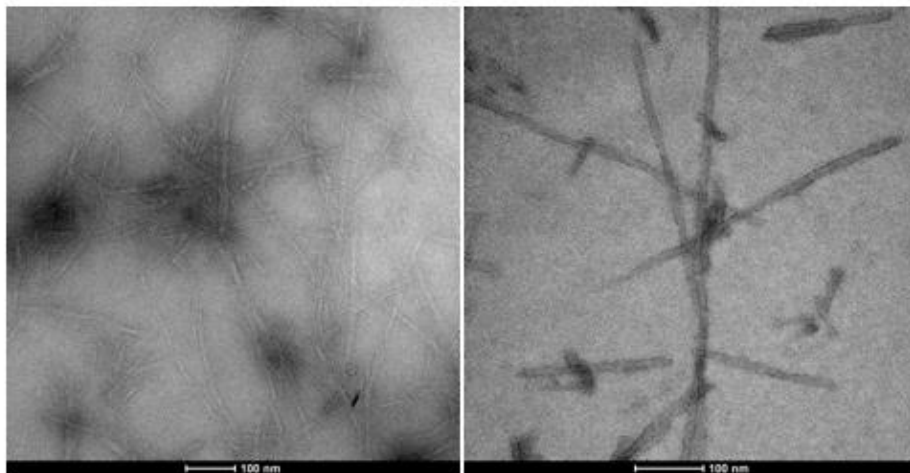
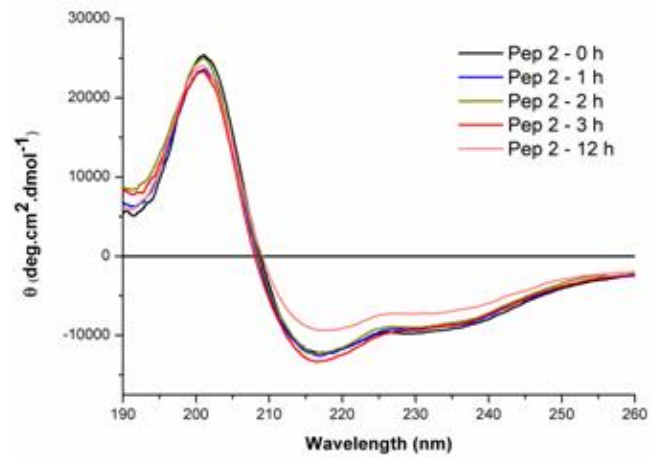


Figure 29. CD Spectrum and TEM images of *Peptide 2* : EFKF-Azo_(3,4)-FKFE (Before UV on the left and after UV on the right side).

Peptides were irradiated with UV-LEDs for 12 hours and their TEM images were taken before and after UV irradiation to see whether a difference between fibrillar structures occurs or not (Figure 27 and 28). Especially for *Peptide 1* TEM images confirm the increase in viscosity of the peptide which is correlated with the increase in β -sheet content determined with CD measurements. On the other hand, for *Peptide 2*, based on TEM images it is hard to say that a large difference occurs upon photoirradiation; however observable macroscopic change in the viscosity of the peptide solution gives hope for the formation of more rigid hydrogels.

After examining potential of hydrogel formation for *Peptide 1* and 2, we extended the chain length to involve 17 amino acids and synthesized *Peptide 3*.

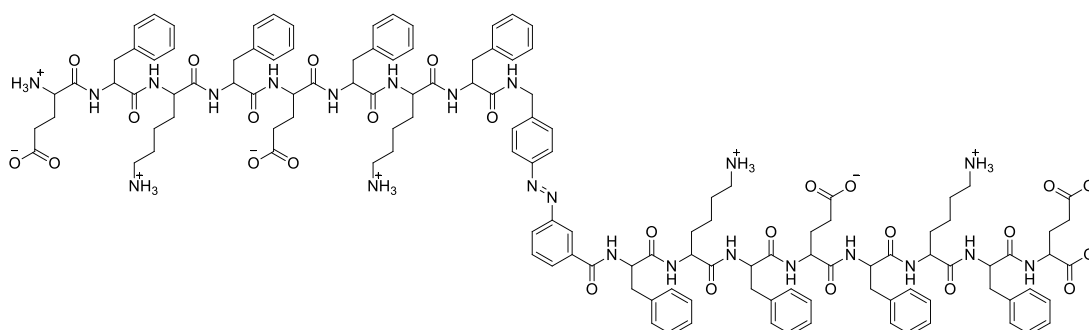


Figure 30. Structure of *Peptide 3* with sequence EFKF EFKF-Azo_(3,4)-FKFEFKFE.

While doing that, we assumed that by increasing hydrophilic groups in peptide backbone, we can increase the possibility of H-bonding and produce more rigid hydrogels. However, after synthesis of this peptide, there has been a solubility problem. Even scanning the solubility conditions at different pH values and in different buffers having same pH gave us no positive result on solubility (Table 4). As a result of this it is decided to change the peptide sequence.

Table 4.Types of buffer and adjusted pH values tested for the solubility of *Peptide 3*.

Type of Buffer	pH
MES	3.0
MES	4.0
MES	5.0
MES	6.0
MES	7.03
HEPES	7.0
Phosphate	7.2
HEPES	8.0

At this stage as an alternative strategy, we wanted to examine the effect of hydrophobicity on hydrogelation of peptides. For that purpose we aimed the decrease of hydrophobic interaction and modified *Peptide 2* and *3* in which phenyl alanines (F) were replaced with lacking aromatic side chain and less hydrophobic alanines (A) (Figure 29).

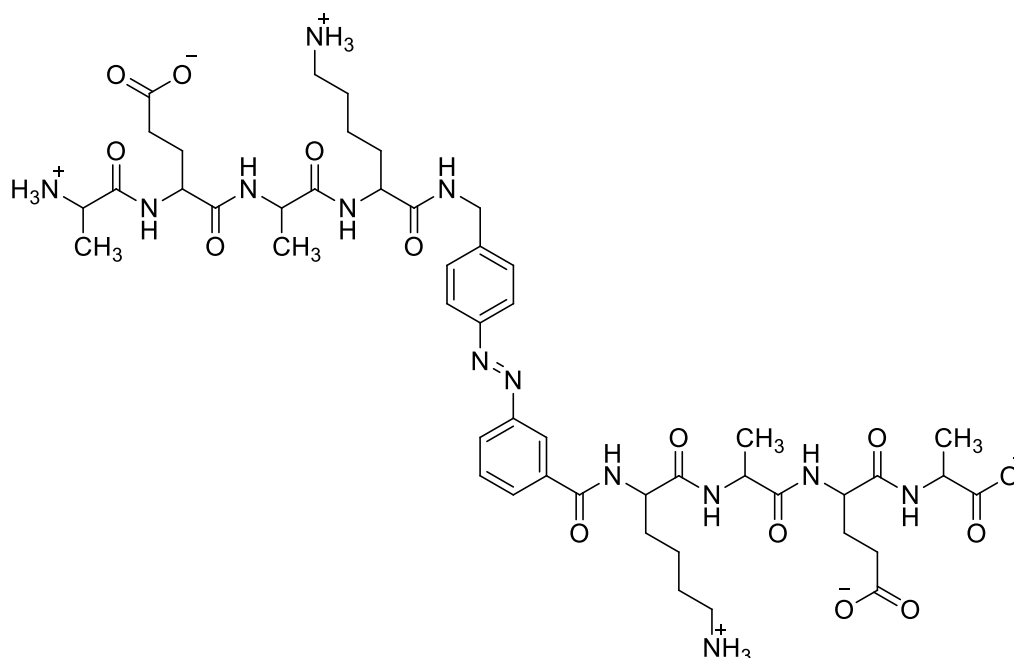


Figure 31.Structure of *Peptide 4* with sequence AEAK-Azo_(3,4)-KAEA.

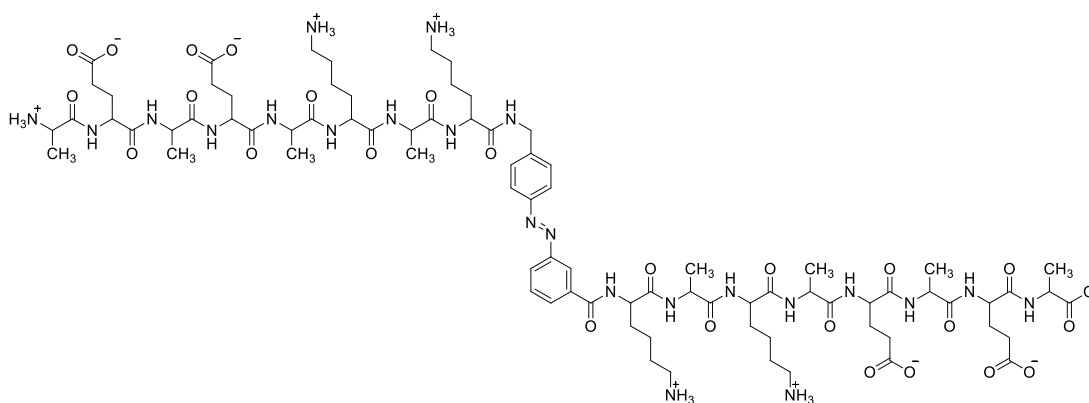


Figure 32. Structure of *Peptide 5* with sequence of AEAEAKAK-Azo_(3,4)-KAKAEAEA.

After facing with the solubility problem of *Peptide 3*, while the phenyl alanines (F) are replaced with alanine (A), this time only Azo_(3,4) artificial amino acid is utilized in the backbone of *Peptide 4* and *5* (Figure 31 and 32) for which the amino acid sequences are listed below (Table 5).

Table 5. Designed peptides for light triggered self-assembly.

	Peptide Sequence	Charge Distribution	Artificial amino acid X
Peptide 1	EFKF-X-FKFE	- + / + -	Azo _(3,3)
Peptide 2	EFKF-X-FKFE	- + / + -	Azo _(3,4)
Peptide 3	EFKFEFKF-X-FKFEFKFE	- + - + / + - + -	Azo _(3,4)
Peptide 4	AEAK-X-KAEA	- + / + -	Azo _(3,4)
Peptide 5	AEAEAKAK-X-KAKAEAEA	- + - + / + - + -	Azo _(3,4)

For the CD measurements, conditions (concentration, temperature and pH) were kept constant but this time, it is determined that *Peptide 4* and *5* had more random coil structures instead of β -sheets (Figure 30 and 31). Especially for *Peptide 4*, since the tendency for random coil formation was increased in time, it did not lead any change in macroscopic appearance of the solution. When the chain length was extended in *Peptide 5* (Figure 32), existing random coil character of the system did not change upon photoirradiation unlike the situation in *Peptide 4*.

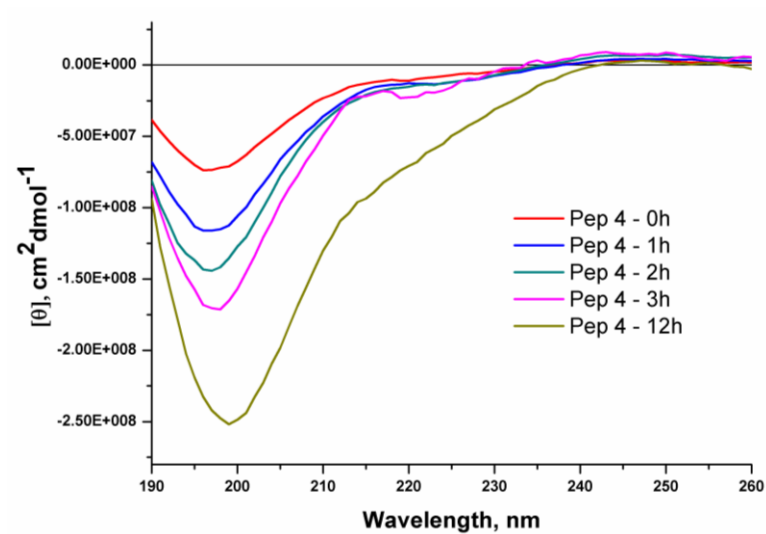


Figure 33. CD spectrum of *Peptide 4*.

For a precise analysis of the secondary structural changes in the system, calculation of the percentages of β -sheet and random coil formations might be necessary. By doing that it would be possible to follow the pattern in change during photoirradiation.

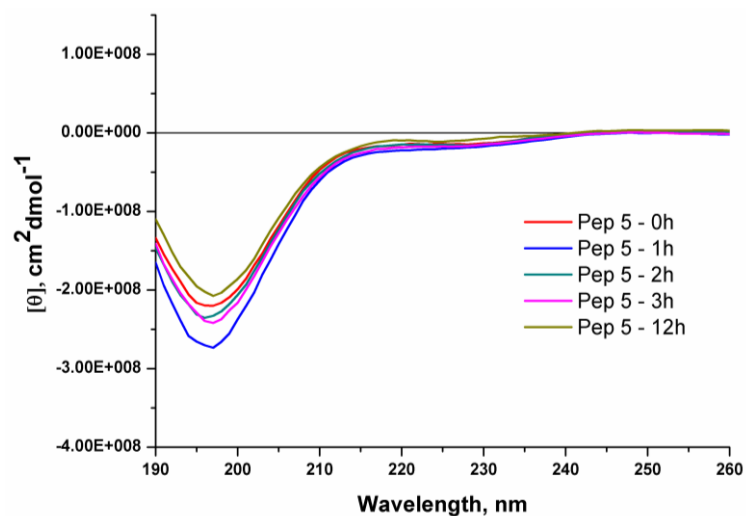


Figure 34. CD Spectrum of *Peptide 5*.

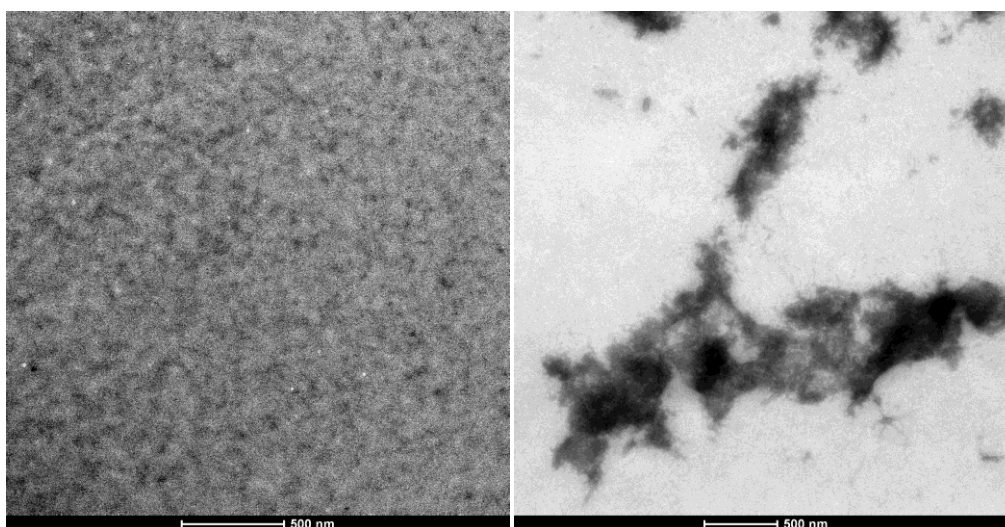


Figure 35.TEM image of *Peptide 5* (before UV irradiation).

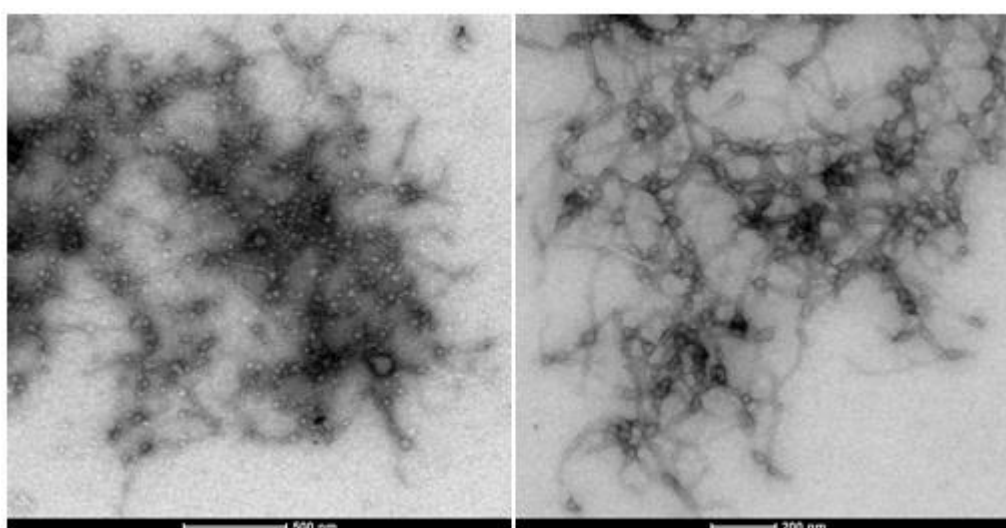


Figure 36.TEM images of *Peptide 5* (after UV irradiation).

TEM measurements were performed for *peptide 5* (Figure 35 and 36) and by comparing these TEM images it can be concluded that while the peptide molecules are dispersed in medium as disordered aggregates, they formed more intertwined fibril-like and additional micelle structures after 12h UV irradiation. When it is looked in general, it can be said that when the secondary structures of peptides deviate from β -sheets, they are forming micelles in addition to bundles. These changes can be investigated more deeply by scanning them in different concentration and with different pH values.

CHAPTER 3

CONCLUSION

To conclude, in this study we tried to achieve light triggered hydrogelation with β -sheet forming peptide sequences incorporated with artificial azobenzene containing amino acids. In order to do that, we studied the effect of chain length, distance between chains and hydrophobicity of the amino acid residues and showed that peptides containing hydrophobic phenyl alanine, hydrophilic lysine and glutamic acid can form β -sheet in their native structures and these can be forced to form more ordered and rigid aggregates upon photoirradiation. *Peptides 1* and *2* could form β -sheet just by dissolving in water. But upon photoirradiation, they turned into more bundled structures which can be considered as the reason of macroscopic change in the appearance of peptide solutions. However, although extension of chain length (*peptide 3*) was aimed to form more rigid β -sheet structures, increasing the number of hydrophobic amino acids caused serious solubility problems.

On the other hand, by changing phenyl alanine with less hydrophobic alanine, it was expected that solubility problem might be solved without significant amount of decrease in hydrogel forming ability of the peptides. But the results showed that substitution of phenyl alanine with less hydrophobic alanine dramatically decreased the β -sheet character of the peptide solution and TEM images showed that they formed micelles in addition to bundled nanotubes. In that step, what could be done is analyzing their β -sheet formations with different pH values. Other than that, alternative peptide sequences can be utilized for testing hydrogel formation which are known as well β -sheet forming peptides. These sequences can include repeating (RADA)_n or (VKVK)_n units in the backbone.

Although it seems that the structural changes of the designed peptides are not sufficient to categorize them as *hydrogel*, the change in their nanostructures upon UV-irradiation gives hope for the production of more rigid gel-like formations.

For their use in biomedical applications as drug delivery agents for example, photoirradiation with 365nm UV- light may seem as a disadvantage for therapeutic applications. However, by coupling them with upconverting nanoparticles, light for photoisomerization can be generated by longer wavelength excitation which can pass through the human skin.³³ This coupling eliminates the damages of UV-light and the system can be used for selective drug delivery.

CHAPTER 4

EXPERIMENTAL

4.1 Materials and Methods

For the synthesis of artificial amino acids, all reactions were monitored by TLC using precoated silica gel plates visualized by UV-light. Final column chromatography separations were performed by silica gel purchased from Aldrich.

Compounds were named by using ChemDraw Ultra 12.0. For the synthesis of pre-designed peptide, all natural amino acids were purchased from ChemImpex.

4.1.1 Nuclear Magnetic Resonance

Nuclear magnetic ($^1\text{H-NMR}$) spectra were recorded in CDCl_3 and $\text{d}^6\text{-DMSO}$ on Bruker Spectrospin Avance DPX 400 spectrometer. Chemical shifts are given in parts per million (ppm) with TMS as internal reference.

4.1.2 HPLC

HPLC purification of the cleaved peptides was performed with Dionex Ultimate 3000 Series equipped with a variable wavelength absorbance detector using a reverse phase C18 column (Hypersil Gold, 12 μm , 250 x 10 mm). A binary gradient of water (0.1% TFA) and acetonitrile (0.1% TFA) was used with a flow rate of 3 mL min^{-1} and the eluent was monitored by UV absorbance at 210, 280, 330 and 450 nm of which two are specific to azobenzene's absorption wavelengths. Fractions were collected and lyophilized after their purity was confirmed by analytical HPLC performed using a RP-C18 column (Acclaim 120, 3 μm , 4.6 x 150 mm) with a flow rate of 0.5 mL min^{-1} .

4.1.3 LC-MS-QTOF

Analytical LC-MS-QTOF analyses of synthetic amino acids and peptides were recorded on an Agilent Technologies High Resolution Mass Quadrupole Time-of-Flight (TOF) LC/MS 1200 series and Zorbax Eclipse XDB-C18 analytical 4.6 x 150 mm 5- micron column was employed. *For the peptides synthesized by SPPS, MS analysis is enough for the characterization of the peptides. No other spectrum such as NMR or IR is needed.*

4.1.4 Photoirradiation

Photoirradiation studies for cis/trans isomerization of synthetic peptides were carried out with a home-made ultra-violet light exposure box composed of 80x1 UV-LEDs and each has a power of 1.0 W distributed to 4 faces of the box.

4.1.5 Circular Dichroism

All CD spectra were recorded in a Jasco J-815 CD spectrophotometer using a circular quartz cuvette with a path length of 1.0 mm from 260 nm to 190 nm at room temperature. The spectra were recorded with an average of three scans at a scan rate of 50 nm/min with a 1 nm step interval and measured in mdeg. 9mM samples were studied in deionized water at a final concentration of 0.18 mM in 1.0 mm cell.

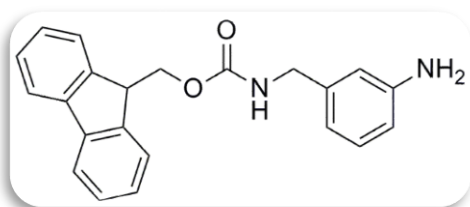
4.1.6 Scanning Electron Microscope

SEM measurements were carried out using Quanta 200 FEG SEM (FEI, Hillsboro, OR) equipped with AmetekApollo X silicon drift detector (EDAX Inc., Mahwah, NJ) with 1 drop of 9 mM samples which were pre-coated with 5 nm Au/Pd alloy.

4.1.7 Transmission Electron Microscope

TEM measurements were carried out using FEI Tecnai G² Spirit BioTwin CTEM Microscope which can enlarge the image up to 340000 times of the original. Samples were first diluted to 1.8 mM and spotted directly (5 μ L) onto carbon coated copper grids, and allowed to stand for 3 minutes. Excess solvent was removed by capillary action (filter paper) and immediately stained with 5 μ L uranyl acetate for 3 minutes. Excess stain was removed and the grids were allowed to dry for overnight.

4.2 Synthesis of (9H-fluoren-9-yl)methyl 3-aminobenzylcarbamate (Compound 1)



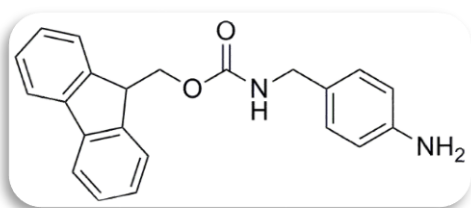
According to synthesis route in literature,³⁴ to the THF/H₂O (1:1) solution, 3-aminobenzyl amine (0.52 g., 4.26 mmol) and NaHCO₃ (0.45 g., 5.36 mmol) were added. Then, Fmoc-OSu (1.1 g., 4.25 mmol) was added in portions over 2h periods in countercurrent of nitrogen gas. The

final mixture was stirred at room temperature for 30 hours. The crude product was precipitated by addition of distilled water and obtained as a yellowish powder with 42 % yield.

^1H NMR (400 MHz, Chloroform-*d*) δ 7.68 (d, $J = 7.5$ Hz, 2H), 7.51 (d, $J = 7.4$ Hz, 2H), 7.31 (t, $J = 7.1$ Hz, 2H), 7.06 – 6.98 (m, 1H), 6.61 – 6.52 (m, 1H), 6.49 (d, $J = 6.1$ Hz, 1H), 4.98 (s, 1H), 4.37 (d, $J = 6.9$ Hz, 2H), 4.20 (d, $J = 5.7$ Hz, 2H), 4.14 (d, $J = 6.5$ Hz, 1H), 3.66 (s, 2H).

^{13}C NMR (100 MHz, CDCl_3) δ 151.7, 142.1, 139.2, 139.01, 136.6, 124.9, 123.1, 122.9, 122.3, 120.3, 120.1, 115.3, 115.2, 63.2, 42.6, 40.1.

4.3 Synthesis of (9H-fluoren-9-yl)methyl 4-aminobenzylcarbamate (Compound 2)



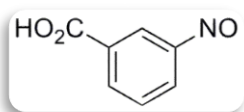
According to synthesis route in literature²⁴, to the THF/ H_2O (1:1) solution 4-aminobenzyl amine (1.1 g., 9.08 mmol) and NaHCO_3 (0.91 g., 10.90 mmol) were added. Then, Fmoc-OSu (3.06 g., 9.08 mmol) was added in portions over 2h period in countercurrent of Nitrogen gas. The

final mixture was stirred overnight at room temperature. Product was precipitated with addition of distilled H_2O , dried via vacuum filtration and obtained as white powder with 96 % yield.

^1H NMR (400 MHz, Chloroform-*d*) δ 7.69 (d, $J = 7.6$ Hz, 2H), 7.51 (d, $J = 7.7$ Hz, 2H), 7.32 (t, $J = 7.5$ Hz, 2H), 7.23 (dt, $J = 8.1, 5.4$ Hz, 2H), 7.00 (d, $J = 8.0$ Hz, 2H), 6.62 – 6.53 (m, 2H), 4.88 (s, 1H), 4.36 (d, $J = 7.0$ Hz, 2H), 4.23 – 4.16 (m, 2H), 4.14 (d, $J = 6.9$ Hz, 1H), 3.61 (s, 2H).

^{13}C NMR (100 MHz, CDCl_3) δ 156.4, 145.9, 144.0, 141.4, 128.9, 128.3, 127.7, 127.2, 125.1, 120.1, 115.2, 66.6, 47.2, 44.8.

4.4 Synthesis of 3-nitrosobenzoic acid (Compound 3)

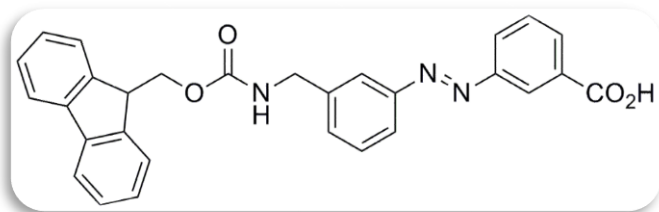


According to synthesis route in literature²⁴, Oxone (9.22 g., 30 mmol) was dissolved in ~ 135 mL distilled H_2O . In another flask, 3-aminobenzoic acid was dissolved in ~ 75 mL DCM. These two solutions were coupled and stirred at room temperature for 3.5 hours. The final nitroso product was precipitated with the addition of distilled H_2O in small portions and vacuum filtrated. For further drying, beige solid was lyophilized. 1.647 g. product was obtained with 80 % yield.

^1H NMR (400 MHz, $\text{DMSO}-d_6$) δ 8.49 – 8.23 (m, 2H), 8.19 (dd, $J = 8.0, 1.4$ Hz, 1H), 7.93 – 7.67 (m, 1H).

^{13}C NMR (100 MHz, DMSO) δ 166.0, 165.7, 136.2, 132.7, 130.5, 124.7, 120.4.

4.4 Synthesis of [3-(3'-(9-Fluorenylmethoxycarbonylamino)methyl)phenylazo]benzoic acid(Compound 4)



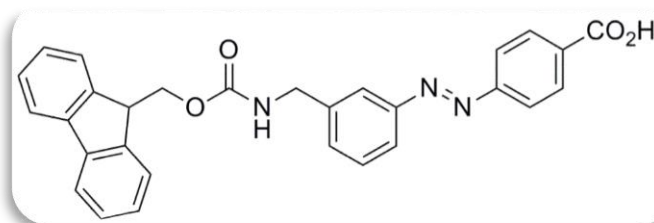
According to synthesis route in literature²⁴, 3-aminobenzoic acid (1.40 g., 9.26 mmol) was added to glacial AcOH/DMSO (1:1) and dissolved well enough. Then, **compound 1** was added.

The reaction mixture was stirred at room temperature for 10 days. After the completion, mixture was filtered off and washed with distilled H₂O in small portions. The crude product was further purified with silica gel column chromatography using DCM/MeOH (9:1) solvent system as eluent. 1.0 g product was obtained with 45 % yield.

¹H NMR (400 MHz, DMSO-*d*₆) δ 8.1 (s, 1H), 7.60 (td, 2H), 7.50 (d, 2H), 7.31-7.16 (m, 12H), 5.20 (dd, 2H), 4.50 (d, 2H), 4.10 (m, 1H) ppm.

¹³C NMR (100 MHz, DMSO) δ 168.5, 156.9, 152.3, 144.2, 141.4, 141.2, 132.4, 130.8, 129.9, 129.8, 129.2, 128.4, 127.7, 127.5, 126.5, 125.6, 122.8, 121.8, 120.5, 119.7, 65.9, 47.2, 43.9.

4.5 Synthesis of [3-(4'-(9-Fluorenylmethoxycarbonylamino)methyl)phenylazo]benzoic acid(Compound 5)



According to synthesis route in literature²⁴, 3-aminobenzoic acid (1.55 g., 10.2 mmol) was dissolved in AcOH/DMSO (1:1) well enough. Then, **compound 2** was added. The reaction mixture

was stirred at room temperature for 52 hours. After the completion, mixture was filtered off and washed with distilled H₂O. The crude product was further purified with silica gel column chromatography using DCM/MeOH (9:1) solvent system as eluent. 954 mg product was obtained with 40 % yield.

¹H NMR (400 MHz, DMSO-*d*₆) δ 8.39 (s, *J* = 1.9 Hz, 1H), 8.11 (ddd, *J* = 9.7, 5.4, 1.6 Hz, 2H), 7.96 (t, *J* = 6.0 Hz, 1H), 7.93 – 7.87 (m, 4H), 7.71 (dd, *J* = 11.3, 7.6 Hz, 3H), 7.43 (t, *J* = 7.5 Hz, 4H), 7.34 (dd, *J* = 8.0, 6.8 Hz, 2H), 4.40 (d, *J* = 6.7 Hz, 2H), 4.29 (d, *J* = 5.9 Hz, 2H), 4.25 (t, *J* = 6.7 Hz, 1H).

¹³C NMR (100 MHz, DMSO) δ 167.7, 156.9, 152.2, 151.3, 144.4, 144.3, 141.2, 132.2, 130.8, 129.9, 128.2, 127.7, 127.5, 127.3, 125.4, 122.7, 121.8, 120.4, 65.8, 47.3, 44.0.

4.6 General Procedure for Solid Phase Peptide Synthesis

Loading first Fmoc-protected amino acid to 2-chlorotriethyl chloride resin:

277 mg (0.25 mmol) resin is weighed in reaction vessel in which the desired peptide will be synthesized. It's washed with DMF (2x) and swelled in 2-3mL DMF for 10-15min. Then, vessel is drained. In a separate scintillation vial, 0.375 mmol Fmoc-Glu(OtBu)-OH is dissolved in 1.5 mL DMF. To this solution, 326 μ L DIEA (1.877 mmol) is added and the solution is transferred to same reaction vessel with resin. After overnight, substitution is checked via UV-spectroscopic methods.³⁵ As a final step, 200 μ L MeOH is added for capping without draining DMF and waited for 30min. Lastly, vessel is drained, washed with DMF (5x) and DCM.

Deprotection:

The Fmoc protecting group is removed by treating the pre-swollen resin with 20% piperidine in DMF for 10 min (2x10 mL). Then the solution is drained and the resin washed with DMF.

Coupling with an Fmoc-protected amino acid:

Fmoc-protected amino acid (0.55 mmol, 5.5 eq.) dissolved in HBTU (1 mL, 0.5 M in DMF) then DIEA (200 μ L) is added. After addition of DIEA, solution is mixed and added to the resin in 30 seconds at max. Mixture is allowed to stand for 1 hour and agitated in every 10 min. Then the solution is filtered off and the resin washed with DMF and DCM. The reaction progress is checked with the Kaiser test.

Final Deprotection:

After deprotection of Fmoc of the very last amino acid residue, resin is washed with DMF (4 \times 2 mL), DCM (4 \times 2 mL) then dried under vacuum.

As an alternative way, final Fmoc deprotection can also be done in solution phase, after cleavage. In order to do that, completely dry powder is dissolved in 20% Piperidine in DMF solution. After the mixture is mixed for 10 min. with sonication, it is precipitated with methyl-*tert*butyl ether. Precipitate is centrifuged and supernatant is poured off. The process is repeated 3-4 times until the supernatant becomes neutral by checking with pH paper.

Cleavage:

98% TFA, 1% DCM and 1% TIPS solution – so called cleavage cocktail – is used to cleave the peptide sequence from resin. This cocktail (2 x 1 mL) added to the resin and waited for 1 hour. Then the solution is collected. The peptide is triturated by addition of ice-cold diethyl

ether and the resulting emulsion is centrifuged at 8500 rpm for 10 min. The solid is filtered off. The product is dissolved in distilled water and lyophilized.

REFERENCES

- [1] Hood, L. & Hunkapiller, T. (1989). Diversity of the Immunoglobulin Gene Superfamily. *Adv. Immunol.*, 44, 1, 1-63.
- [2] Bender, M.L.; Bergeron, R.J. & Komiyama, M. (1984). *The Bioorganic Chemistry of Enzymatic Catalysis*. Wiley, New York.
- [3] Kitai, R.; Ryle, A.P. & Sanger, F. (1955). The disulphide bonds of insulin. *Biochem. J.*, 60, 541-556.
- [4] Behrens, O.K.; Bromer, W.W. & Sinn, L.G. (1956). The Amino Acid Sequence of Glucagon. *J. Am. Chem. Soc.*, 78, 3858 – 3860.
- [5] Jakubke, H.D. & Sewald, N. (2009). *Peptides: Chemistry and Biology*. Weinheim: WILEY-VCH (Second, Revised and Updated Edition). Chp3.
- [6] Ramachandran, G. N., Ramakrishnan, C., & Sasisekharan, V. (1963). Stereochemistry of Polypeptide Chain Conformations. *Journal of Molecular Biology*, 7 (1), 95-99.
- [7] Dasgupta, A., Mondal, J., & Das, D. (2013). Peptide hydrogels. *RSC Advances*, 3, 9117-9149.
- [8] Zhang, S., Holmes, T., Lockshin, C., & Rich, A. (1993). Spontaneous assembly of a self-complementary oligopeptide to form a stable macroscopic membrane. *Proc. Natl. Acad. Sci. USA*, 90, 3334-3338.
- [9] Cui, H., Webber, M., & Stupp, S. (2010). Self-Assembly of Peptide Amphiphiles: From Molecules to Nanostructures to Biomaterials. *Peptide Science*, 94, 1-18.
- [10] Bechhoefer, J.; Chen, P.; Ha, B.-Y.; Hong, Y.; Imamura, H. & Jun, S. (2004). Self-Assembly of the Peptide EAK16: The Effect of Charge Distributions on Self-Assembly. *Biophysical Journal*, 87(2), 1249-1259.
- [11] Holmes, T.C.; Lockshin, C. & Rich, A. (1993). Spontaneous Assembly of a Self-Complementary Oligopeptide to Form a Stable Macroscopic Membrane. *Proc. Natl. Acad. Sci.*, 90, 3334-3338.

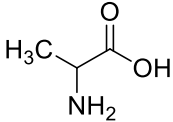
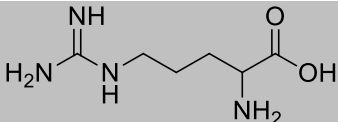
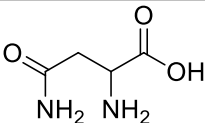
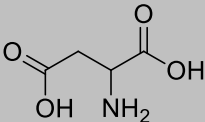
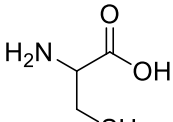
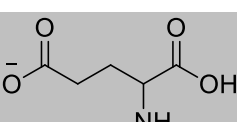
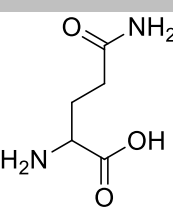
- [12] Sun, S. & Bernstein, E.R. (1996). Aromatic van der Waals Clusters: Structure and Nonrigidity. *J. Phys. Chem.*, 100, 13348-13366.
- [13] Bowerman, C.J.; Nilsson, B.L.; Nissan, D.A. & Ryan, D.M. (2009). The Effect of Increasing Hydrophobicity on the Self-Assembly of Amphipathic β -Sheet Peptides. *Mol. BioSyst.*, 5, 1058-1069.
- [14] Uljin, R., & Smith, A. (2008). Designing Peptide Based Nanomaterials. *Chemical Society Reviews*, 37, 664-675.
- [15] Löwik, D., Leunissen, E., Van den Heuvel, M., Hansen, M., & Van Hest, J. (2010). Stimulus responsive peptide based materials. *Chem. Soc. Rev.*, 39, 3394-3412.
- [16] Boweman, C., & Nilsson, B. (2010). A Reductive Trigger for Peptide Self-Assembly and Hydrogelation. *J. Am. Chem. Soc.*, 132, 9526-9527.
- [17] Branco, M.C., Knerr, P.J., Micklitsch, C.M., Nagarkar, R., Pochan, D.J., & Schneider, J.P. (2011). Zinc-Triggered Hydrogelation of a Self-Assembling b-Hairpin Peptide. *Angew. Chem. Int. Ed.*, 50, 1577–1579.
- [18] Haines, L.A., Ozbas, B., Pochan, D.J., Rajagopal, K., Salick, D.A., & Schneider, J.P. (2005). Light Activated Hydrogel Formation via the Triggered Folding and Self-Assembly of a Designed Peptide. *J. Am. Chem. Soc.*, 127, 17025-17029.
- [19] Merrifield, B.M. (1963). Solid Phase Peptide Synthesis. I. The Synthesis of a Tetrapeptide. *J. Am. Chem. Soc.*, 85, 2149-2154.
- [20] Griffiths, J. (1972). Photochemistry of Azobenzene and its Derivatives. *J. Am. Chem. Soc.*, 1, 4, 481-493.
- [21] Beveridge, D.L. & Jaffer, H.H. (1966). The Electronic Structure and Spectra of cis- and trans-Azobenzene. *J. Am. Chem. Soc.*, 88, 1948-1953.
- [22] Kroner, J. & Bock, H. (1968). Azo-Verbindungen, IX. Hückel-MO-Rechnungen an Dialkylamino- und Nitro-azobenzolen. *Chem. Ber.*, 101, 1922-1932.
- [23] Jaffer, H.H.; Yeh, S.J. & Gardner, R.W. (1958). The electronic spectra of Azobenzene derivatives and their conjugate acids. *J. Mol. Spectroscopy*, 2, 120- 136.
- [24] Zollinger, H. (2003). Color Chemistry, Syntheses, Properties, and Applications of Organic Dyes and Pigments. Weinheim: WILEY-VCH (3rd edition). Pg: 37-38.

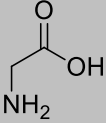
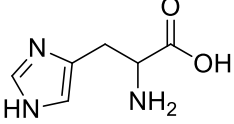
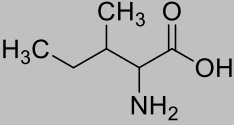
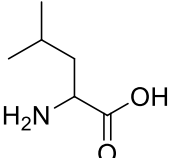
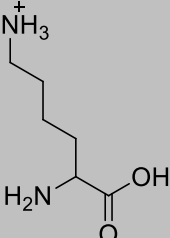
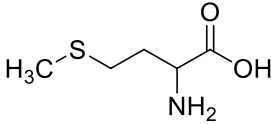
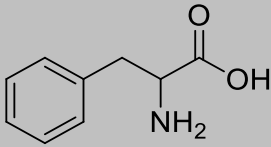
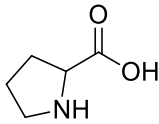
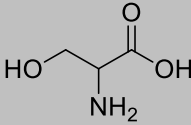
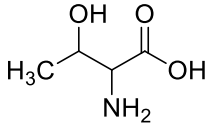
- [25] Asano, T.; Kusano, Y.; Manabe, O.; Okada, T.; Shigematsu, K. & Shinkai, S. (1981). Temperature and Pressure Dependences of Thermal Cis-to-Trans Isomerization of Azobenzenes Which Evidence an Inversion Mechanism. *J. Am. Chem. Soc.*, 103, 5161-5165.
- [26] Rau, H. In *Photochemistry and Photophysics*; Rabek, J.F., Ed.; CRC Press: Boca Raton, FL, 1990; Vol.2, Chapter 4.
- [27] Dou, Y.; Lei, Y.; Shao, J.; Wang, Z. & Wen, Z. (2008). Non-adiabatic Simulation of Photoisomerization of Azobenzene: Detailed Mechanism and Load-Resisting Capacity. *J. Chem. Phys.*, 129, 164111(1-9).
- [28] Beharry, A.A. & Woolley, A. (2011). Azobenzene Photoswitches for Biomolecules. *Chem. Soc. Rev.*, 40, 4422-4437.
- [29] Huang, Y.; Lin, H.; Shi, J.; Qiu, Z.; Xu, Yanmei & Zhang, Y. (2011). Supramolecular Hydrogels Based on Short Peptides Linked with Conformational Switch. *Org. Biomol. Chem.*, 9, 2149-2155.
- [30] Aemissegger, A.; Gunsteren, W.F.; Hilvert, D. & Kräutler, D. (2004). A Photoinducible β -Hairpin. *J. Am. Chem. Soc.*, 127, 2929-2936.
- [31] Barret, C.J.; Halabieh, R.H. & Mermut, O. (2004). Using Light to Control Physical Properties of Polymers and Surfaces with Azobenzene Chromophores. *Pure Appl. Chem.*, 76, 1445-1465.
- [32] Kelly, S.M. & Price, N.C. (2000). The Use of Circular Dichroism in the Investigation of Protein Structure and Function. *Current Protein and Peptide Science.*, 349-384.
- [33] Haase, M. & Schafer, H. (2011). Upconverting Nanoparticles. *Angew. Chem. Int. Ed.*, 50, 5808-5829.
- [34] Priewisch, B. (2006). Photoswitchable Amino Acids – Synthesis, Photochromism and Incorporation into Peptidic Grb2-SH2 Antagonists. (Published doctoral dissertation). Technische Universität Berlin, Berlin, Germany.
- [35] *Tips for peptide synthesis.* (n.d.). Retrieved from http://www.anaspec.com/html/peptide_tips.html

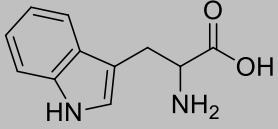
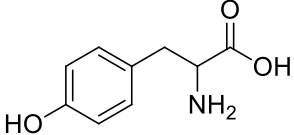
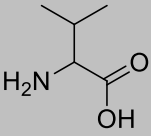
APPENDIX A

LIST OF 21 AMINO ACIDS FOUND IN NATURE

Table A.1

Name	3-Letter code	1-Letter code	Structure
Alanine	Ala	A	
Arginine	Arg	R	
Asparagine	Asn	N	
Aspartic acid	Asp	D	
Cysteine	Cys	C	
Glutamic acid	Glu	E	
Glutamine	Gln	Q	

Glycine	Gly	G	
Histidine	His	H	
Isoleucine	Ile	I	
Leucine	Leu	L	
Lysine	Lys	K	
Methionine	Met	M	
Phenylalanine	Phe	F	
Proline	Pro	P	
Serine	Ser	S	
Threonine	Thr	T	

Tryptophan	Trp	W	
Tyrosine	Tyr	Y	
Valine	Val	V	

APPENDIX B

HR-MS PROFILES

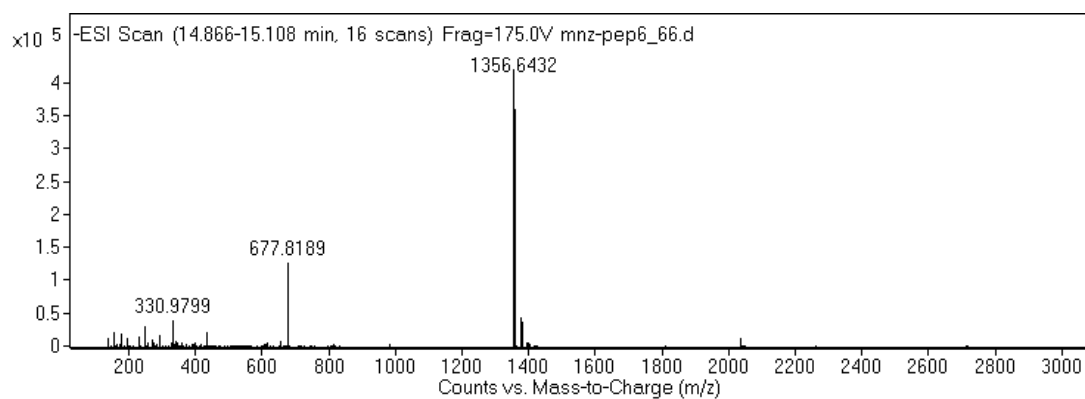


Figure B.1 QTOF-ESI-MS spectrum of *Peptide 1*

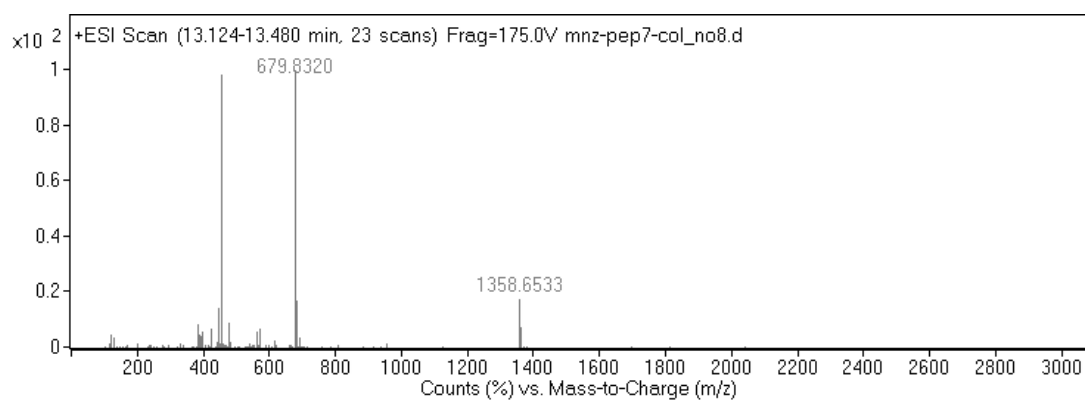


Figure B.2 QTOF-ESI-MS spectrum of *Peptide 2*

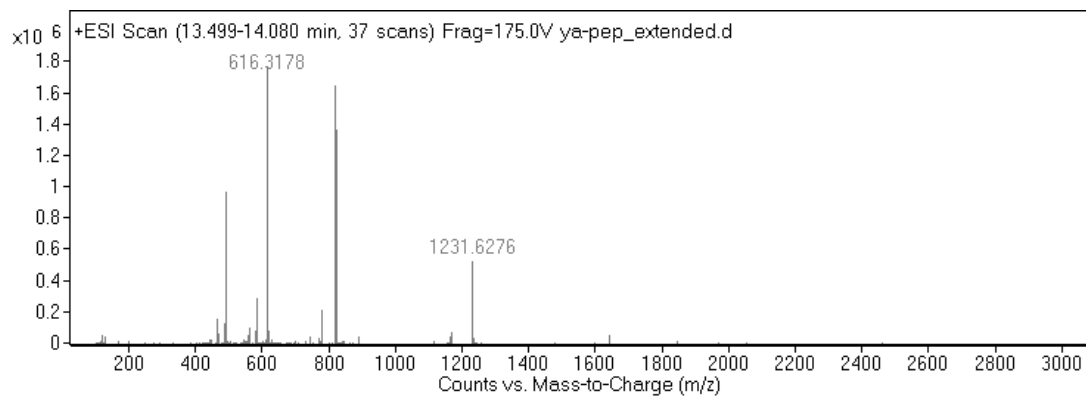


Figure B.3 QTOF-ESI-MS spectrum of crude *Peptide 3*

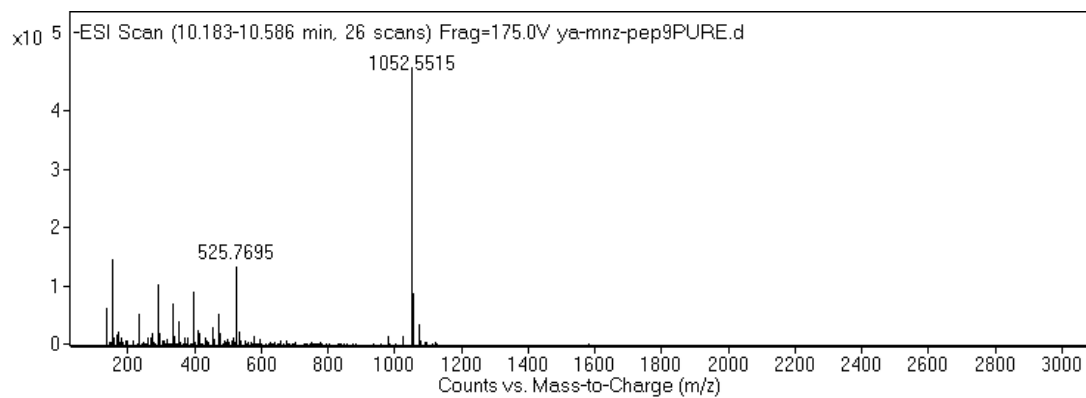


Figure B.4 QTOF-ESI-MS spectrum of *Peptide 4*

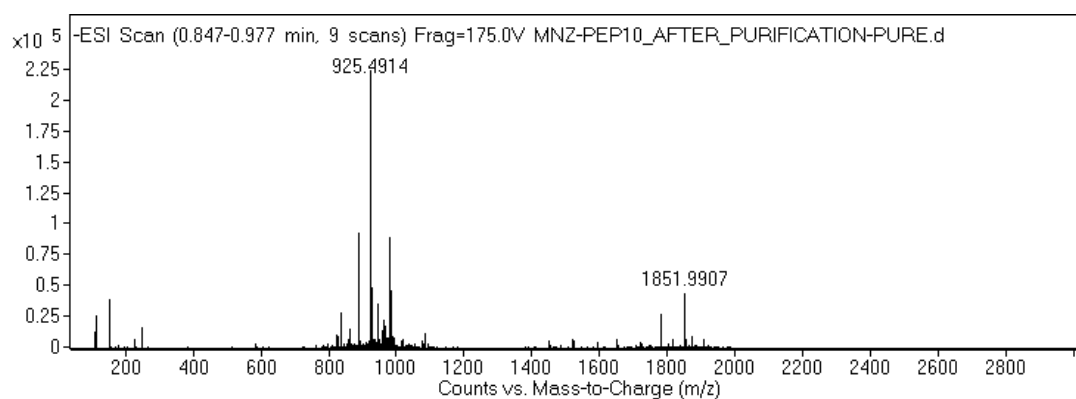


Figure B.5 QTOF-ESI-MS spectrum of *Peptide 5*

APPENDIX C

HPLC PROFILES

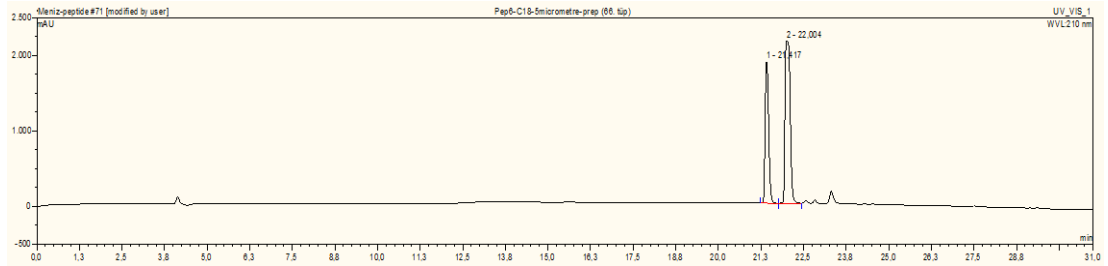


Figure C.1 HPLC Spectrum of *Peptide 1* at 210 nm

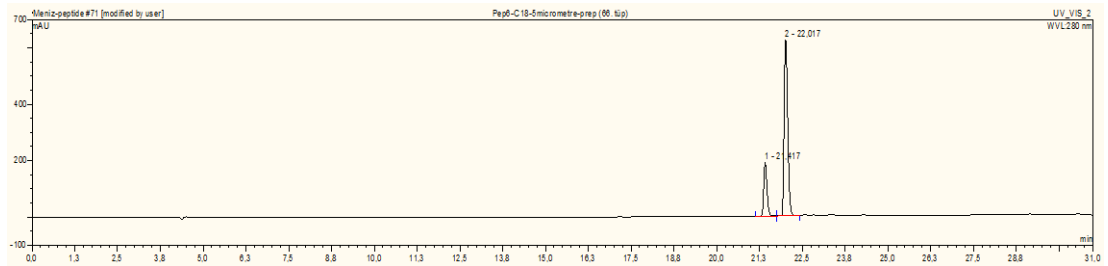


Figure C.2 HPLC Spectrum of *Peptide 1* at 280 nm

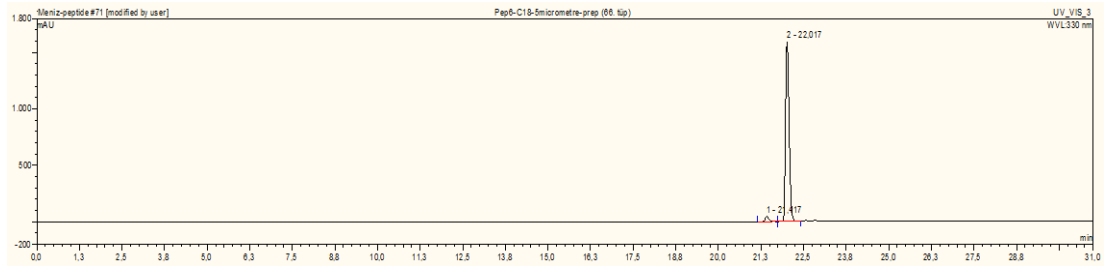


Figure C.3 HPLC Spectrum of *Peptide 1* at 330 nm

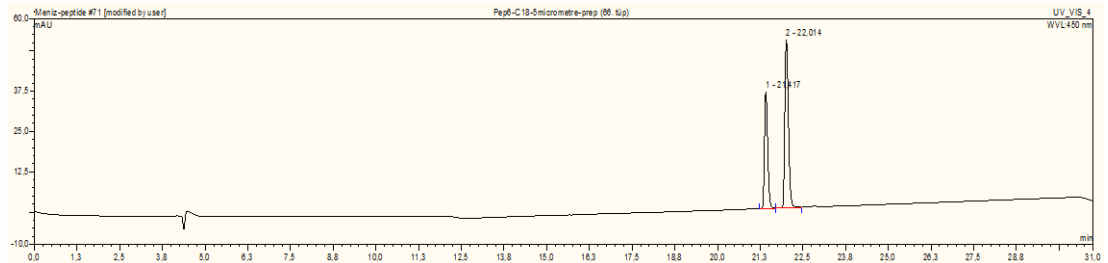


Figure C.4 HPLC Spectrum of *Peptide 1* at 450 nm

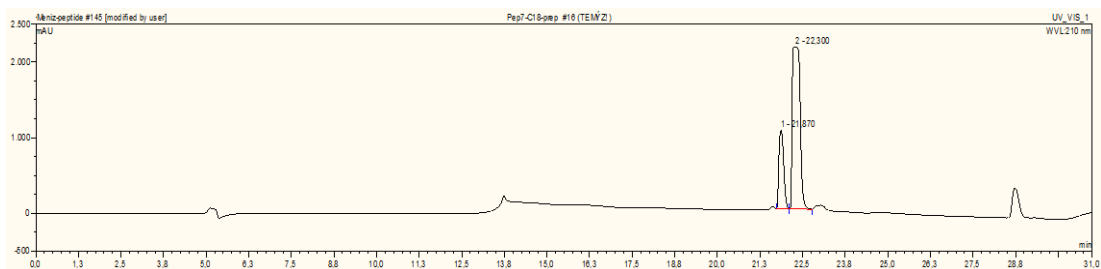


Figure C.5 HPLC Spectrum of *Peptide 2* at 210 nm

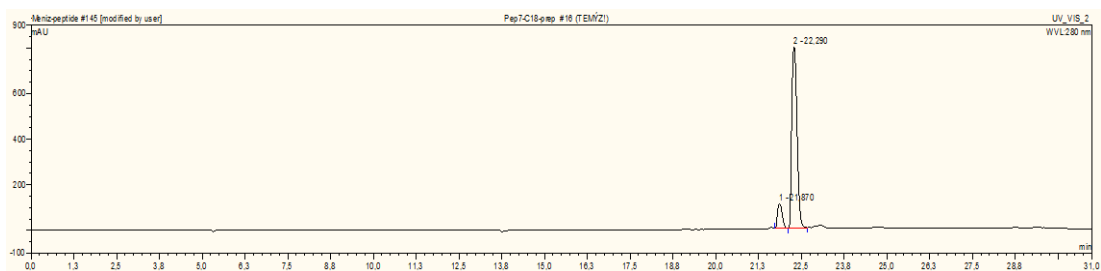


Figure C.6 HPLC Spectrum of *Peptide 2* at 280 nm

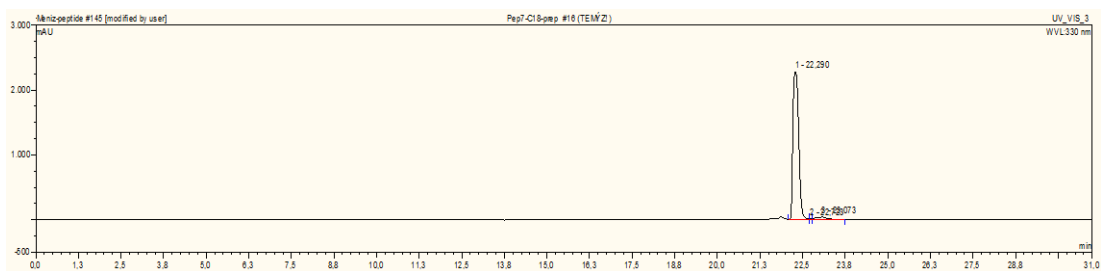


Figure C.7 HPLC Spectrum of *Peptide 2* at 330 nm

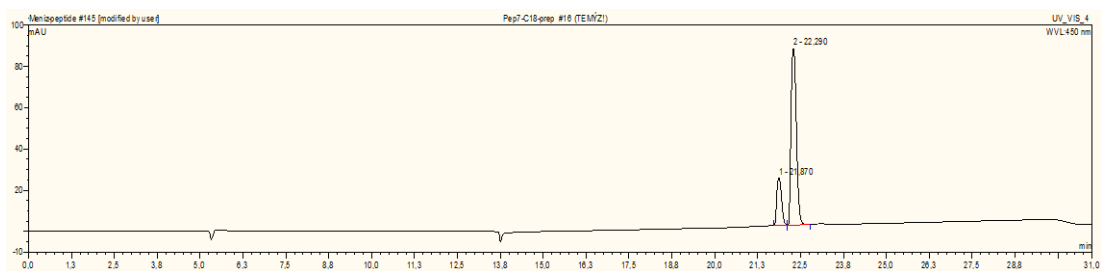


Figure C.8 HPLC Spectrum of *Peptide 2* at 450 nm

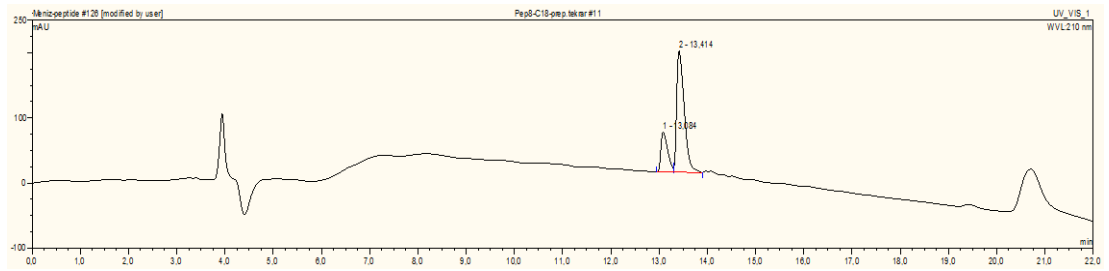


Figure C.9 HPLC Spectrum of *Peptide 3* at 210 nm

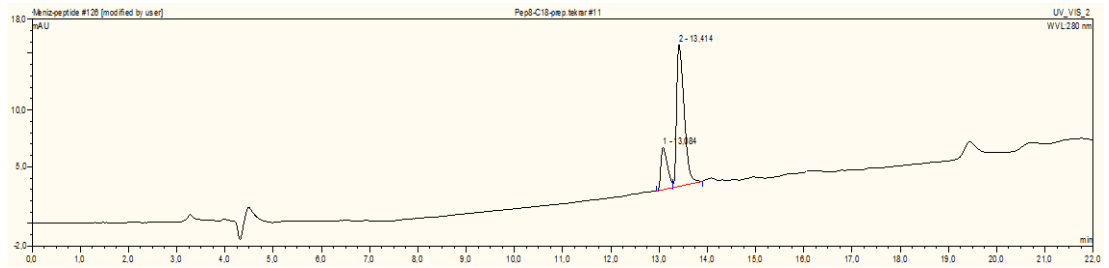


Figure C.10 HPLC Spectrum of *Peptide 3* at 280 nm

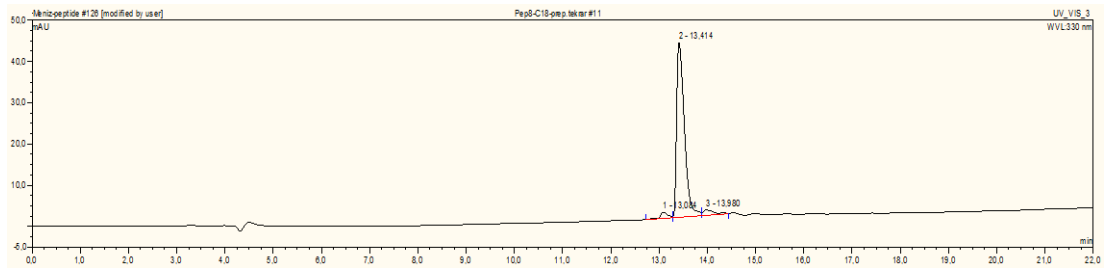


Figure C.11 HPLC Spectrum of *Peptide 3* at 330 nm

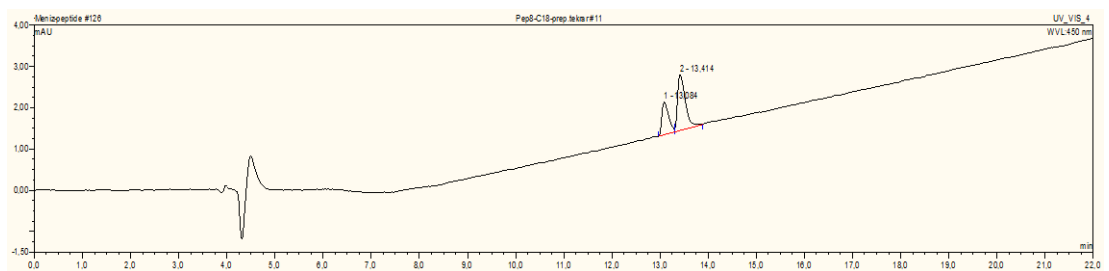


Figure C.12 HPLC Spectrum of *Peptide 3* at 450 nm

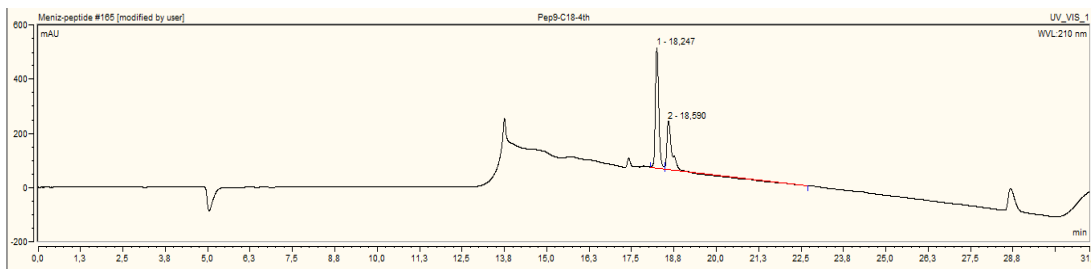


Figure C.13 HPLC Spectrum of *Peptide 4* at 210 nm

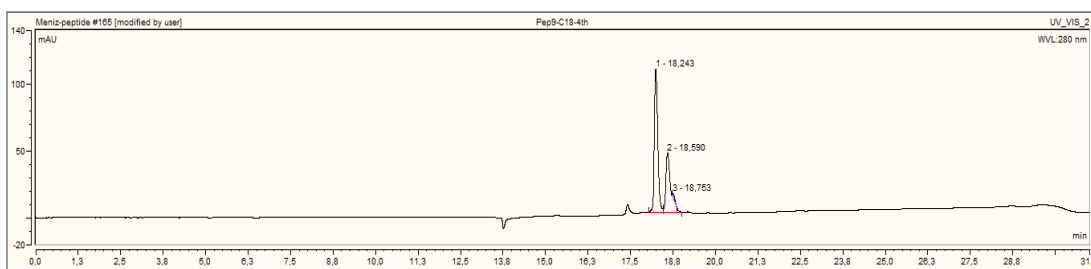


Figure C.14 HPLC Spectrum of *Peptide 4* at 280 nm

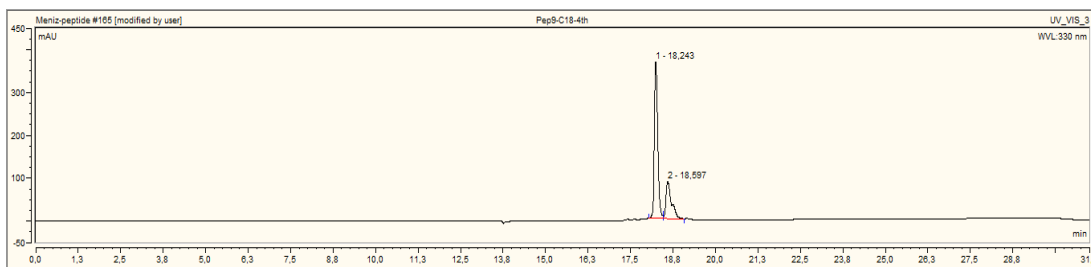


Figure C.15 HPLC Spectrum of *Peptide 4* at 330 nm

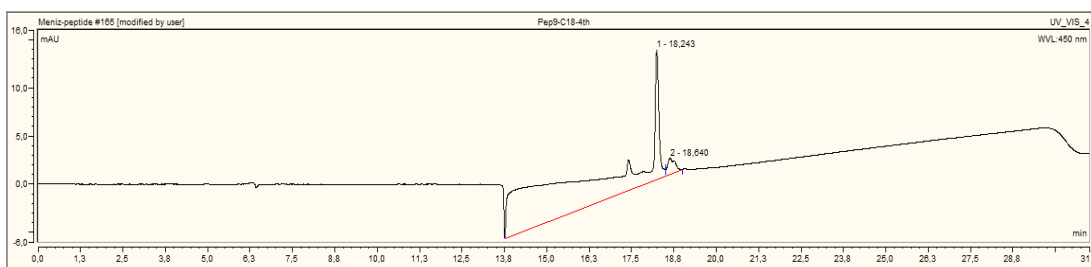


Figure C.16 HPLC Spectrum of *Peptide 4* at 450 nm

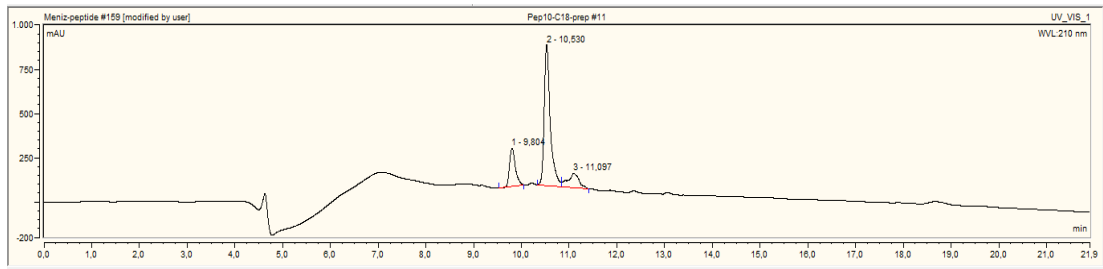


Figure C.17 HPLC Spectrum of *Peptide 5* at 210 nm

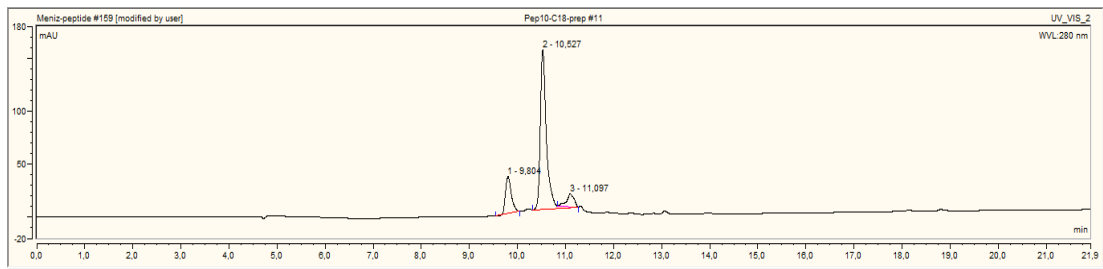


Figure C.18 HPLC Spectrum of *Peptide 5* at 280 nm

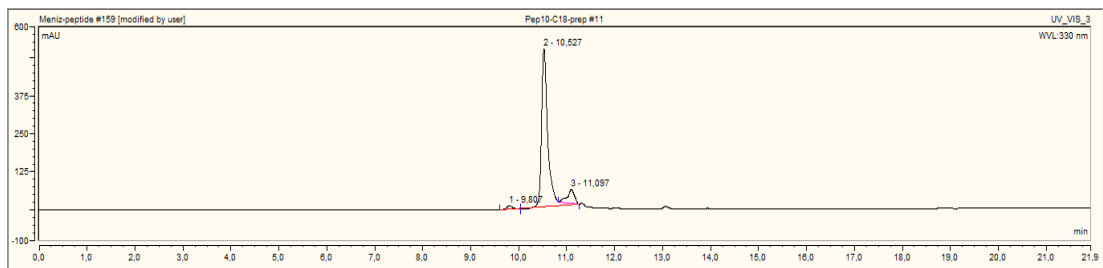


Figure C.19 HPLC Spectrum of *Peptide 5* at 330 nm

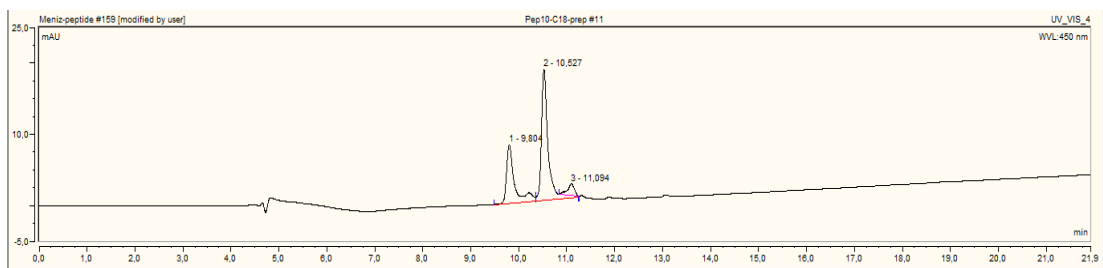


Figure C.20 HPLC Spectrum of *Peptide 5* at 450 nm